Computers in Biology and Medicine 195 (2025) 110597

Contents lists available at ScienceDirect

Computers in Biology and Medicine

journal homepage: www.elsevier.com/locate/compbiomed

Empowering heart attack treatment for women through machine learning and optimization techniques

Doaa Sami Khafaga [a], Marwa M. Eid [b,c], El-Sayed M. El-kenawy [d,e], Ehsaneh Khodadadi [f], Amel Ali Alhussan [a], Nima Khodadadi [g,*]

[a] Department of Computer Sciences, College of Computer and Information Sciences, Princess Nourah bint Abdulrahman University, P.O. Box 84428, Riyadh 11671, Saudi Arabia
[b] Faculty of Artificial Intelligence, Delta University for Science and Technology, Mansoura 11152, Egypt
[c] Jadara University Research Center, Jadara University, Jordan
[d] School of ICT, Faculty of Engineering, Design and Information and Communications Technology (EDICT), Bahrain Polytechnic, PO Box 33349, Isa Town, Bahrain
[e] Applied Science Research Center, Applied Science Private University, Amman, Jordan
[f] Department of Chemistry and Biochemistry, University of Arkansas, Fayetteville, AR, 72701, USA
[g] Department of Civil and Architectural Engineering, University of Miami, Coral Gables, FL, USA

ARTICLE INFO

Dataset link: https://www.kaggle.com/datasets/rashikrahmanpritom/heart-attack-analysis-prediction-dataset

Keywords:
Heart attack treatment
Machine learning
Waterwheel plant algorithm
Stochastic Fractal Search

ABSTRACT

Heart attack detection and treatment in women remain significantly under-optimized due to differences in symptom presentation and physiological characteristics compared to men, leading to delayed or incorrect diagnoses. Addressing this gap, this study introduces an optimized ensemble learning approach that leverages a novel voting classifier combining the Waterwheel Plant Algorithm (WWPA) with Stochastic Fractal Search (SFS). The proposed WWPA+SFS model is designed to enhance the accuracy of heart attack classification in women by integrating multiple machine learning classifiers, including Gaussian Naive Bayes, Random Forest, Logistic Regression, Stochastic Gradient Descent Classifier, Support Vector Classifier, Decision Tree, and k-nearest Neighbors. A comprehensive clinical dataset comprising 303 patient records and 14 features—covering demographic data, exercise-induced angina, chest pain type, major vessel count, cholesterol levels, fasting blood sugar, and resting electrocardiographic results—was used for evaluation. The model's performance was validated using 10-fold cross-validation, Analysis of Variance (ANOVA), and the Wilcoxon Signed Rank Test, benchmarking it against other optimization-based classifiers such as Grey Wolf Optimization (GWO), Whale Optimization Algorithm (WOA), Particle Swarm Optimization (PSO), and Genetic Algorithm (GA). The proposed WWPA+SFS model achieved the highest classification accuracy (97.01%) and demonstrated low variance across multiple trials. These results underline the robustness and effectiveness of the proposed method in optimizing diagnostic models for women's cardiovascular care, potentially reducing misdiagnosis rates, lowering healthcare costs, and contributing to personalized treatment advancements in clinical practice.

1. Introduction

Heart attacks are a global healthcare burden, and treatment can be costly. This initiative can lower heart attack healthcare costs by enhancing diagnosis and treatment. Improving the effectiveness of heart attack identification in women can result in a diagnosis that is both more accurate and timelier, which would save lives. When it comes to heart attacks, women have received an incorrect diagnosis since their symptoms are different from men's experiences [1,2]. Ischemic heart disease (IHD) is the primary cause of illness and death in both males and females. However, young women experience the most severe outcomes, which is likely due to the more intricate range of IHD in women compared to men [3]. The analysis in [4] encompassed a cohort of 607 women actively participating in the Women's Ischemia Syndrome Evaluation (WISE) original cohort and had accessible HDL-C measurements. This study employed multivariate Cox proportional hazard regression and spline regression analysis to assess the associations between HDL-C levels and various outcomes. During the 20th century, cardiovascular disease (CVD) was mostly associated with men. In contrast, women were thought to be shielded from it before menopause due to natural hormones and after menopause through hormone therapy [5]. Heart attacks affect the healthcare systems worldwide significantly, and the related costs of treatment and rehabilitation can be substantially high.

* Corresponding author.
E-mail address: Nima.khodadadi@miami.edu (N. Khodadadi).

https://doi.org/10.1016/j.compbiomed.2025.110597
Received 12 May 2025; Received in revised form 16 June 2025; Accepted 16 June 2025

By improving diagnosis and treatment, this research can help reduce the total cost of the healthcare requirements related to heart attacks. About 5 million women ran businesses when the pandemic started in February [6].

Artificial Intelligence (AI) and machine learning could transform healthcare. Data and analytics can help healthcare practitioners make better decisions, which enhances patient outcomes and can help allocate resources better. The study in [7] examines and compares various artificial intelligence techniques, including logistic regression, Naïve Bayes, K-nearest neighbor (K-NN), support vector machine (SVM), decision tree, random forest, multilayer perceptron (MLP), two distinct types of heart disease datasets: one containing all features and the other containing selected features. To conduct variable selection on a dataset consisting of 1227 baseline Women's Health Initiative (WHI) variables related to the primary outcome of incident Heart failure (HF), two machine-learning techniques, namely Least Absolute Shrinkage and Selection Operator (LASSO) and Classification and Regression Trees (CART), were employed [8]. The accuracy of heart disease predictions was improved in [9] by deploying several machine learning and deep learning classifiers, including K-NN, SVM, Convolutional Neural Network, Logistic Regression, XGBoost, Gradient Boost, and Random Forest. The study investigated various classifiers and evaluated their efficacy, offering significant insights for developing resilient prediction models for myocardial infarction.

Beyond cardiovascular prediction, recent research also explores AI and deep learning for broader medical diagnostics. For example, brain tumor prediction using MRI scans has been investigated through comparative deep learning models [10]. Edge-guided filtering for CT image denoising using fractional order total variation has shown promise in improving diagnostic image quality [11]. Efficient medical image-based reversible data hiding using singular value decomposition (SVD) on denoised images further enhances secure data management in healthcare [12]. Other works have focused on COVID-19 CT image denoising using convolutional neural networks and method noise thresholding [13], and multiscale feature scaling with deep neural networks for brain tumor classification in MRI images [14]. These studies underscore the growing scope of AI-driven methods across medical imaging and diagnostic tasks, reinforcing the relevance and transferability of such methods to cardiovascular applications.

Digital acquisition and analysis are crucial to diagnostic capacities, especially cardiovascular imaging. As a bonus, using AI in digital cardiovascular imaging has dramatically increased the scope of possible advancements [15]. Constantly locating the optimal solution in a vast search space is a challenge that requires refinement. Optimization is the process of locating the optimal solution without employing brute-force criteria. The objective of the optimization is to decrease the number of potential solutions by implementing exploration and exploitation tactics. The optimization strategy accomplishes the objective function and delivers the optimal solution in a reasonable time by utilizing metaheuristics and evolutionary algorithms. Metaheuristic and evolutionary optimization algorithms traverse the search space efficiently to ensure that local optima do not constrain the best solution. These optimization algorithms have demonstrated their efficacy in resolving diverse problem types across various domains and applications, such as engineering [16], economics [17], transportation [18], and mechanics [19]. Recently, various metaheuristic and evolutionary optimization algorithms have been demonstrated to resolve various problems. Notable examples of such algorithms are particle swarm optimization (PSO) [20], Divine religions algorithm (DRA) [21], gravitational search algorithm (GSA) [22], grey wolf optimization algorithm (GWO) [23], Al-Biruni Earth Radius (BER) [24], genetic algorithm (GA) [25], Waterwheel plant algorithm (WWPA) [26], Puma optimizer (PO) [27], Hippopotamus Optimization (HO) [28], Electric eel foraging optimization (EEFO) [29], Tianji's horse racing optimization (THRO) [30], and Stochastic paint optimizer (SPO) [31].

This work can enhance healthcare research based on AI, making healthcare systems more efficient and effective, which could change women's lives. This research uses recent technology and optimization algorithms to improve heart attack diagnostic accuracy in a minimum time and at a lower cost, which can improve patient and healthcare system outcomes. The social benefits of this research are significant and can be far-reaching. By improving the accuracy of heart attack detection and classification in women, this work can save lives and improve quality of life, reducing healthcare costs and participating in healthcare research. These social benefits can ultimately contribute to a healthier and happier society. In addition to saving women's lives, this work can help reduce healthcare costs related to heart attacks. Employing machine learning, and consequently AI, in healthcare has the potential to revolutionize the field of heart attack classification. By using the power of collected data and applying recent data analytics algorithms, healthcare professionals can benefit from this to make more informed decisions, improving patient outcomes and allocating resources in better ways. This work can contribute effectively to the growing body of medical research on the use of AI in healthcare, which consequently helps to pave the way for more efficient and effective healthcare systems in the future.

The social benefits of this research work are mainly in the potential impact on women's lives. By proposing innovations in the fields of metaheuristic optimization and cardiovascular imaging, the proposed voting classifier based on the WWPA algorithm combined with the Stochastic Fractal Search (SFS) algorithm using various machine learning models such as Random Forest, Logistic Regression, Stochastic Gradient Descent Classifier, Support Vector Classifier, and k-Nearest Neighbors. The work aims to improve the accuracy of heart attack detection and classification in women, which can lead to the following social benefits:

1. Reducing Mortality Rates: One of the most significant benefits of this research is its potential to reduce death rates among women. Early detection and classification of heart attacks can achieve that by allowing for timely medical intervention. By improving the accuracy of heart attack detection, the current work can help reduce the number of deaths caused by heart attacks in women.
2. Improving Quality of Life: Heart attacks can severely impact the quality of life for some people, even for surviving ones. By improving the accuracy of heart attack detection and classification, this research can ensure that women receive the appropriate treatment and support effectively in their need to manage their condition. For women who experience heart attacks, this can lead to improved life quality.
3. Reducing Healthcare Costs: Heart attacks financially burden healthcare systems worldwide and affect people significantly. Improving heart attack detection and classification accuracy can help reduce the cost of healthcare concerning heart attacks. This can make healthcare more accessible and affordable for women.
4. Advancing Healthcare Research: The proposed voting classifier algorithm (WWPA+SFS) has the potential to make an effective contribution to the field of healthcare research. By contributing more knowledge on heart attacks in women, this work will help improve healthcare outcomes for all patients, especially women. This can lead to better patient care and more effective healthcare systems overall.

This work presents a novel voting classifier (WWPA+SFS) that combines the Waterwheel Plant Algorithm (WWPA) with Stochastic Fractal Search (SFS). The proposed voting classifier is built based on various machine learning models, including Gaussian Naive Bayes (Gaussian NB), Random Forest (RF), Logistic Regression (LR), Stochastic Gradient Descent Classifier (SGDC), Decision Tree (DT), Support Vector Classifier (SVC), and k-NN. The tested dataset in this work includes a comprehensive health parameter for a set of patients. These parameters include

Table 1
Comparing the recent work related to heart disease.

No.	Main Focus	Methodology	Key Findings
Ref. [32]	Construction of an AI-based heart disease detection system using ML algorithms.	Development of a Python-based application for healthcare research, logistic regression, and random forest classifier algorithm.	Achieved approximately 83% accuracy in heart disease detection using ML.
Ref. [33]	Utilization of ML in predicting heart diseases through health monitoring with wearable sensors.	Implementation of various ML algorithms for heart disease prediction.	Logistic regression with majority voting attained 88.59% accuracy in heart disease prediction.
Ref. [34]	Proposal of a sequential feature selection (SFS) algorithm for detecting death events in heart disease patients.	Application of SFS algorithm for feature selection and comparison with various ML algorithms.	Random Forest Classifier_FS achieved 86.67% accuracy using the SFS method.
Ref. [35]	Evaluation of ML techniques in subtype classification and risk prediction across heart failure, acute coronary syndromes, and atrial fibrillation.	Rigorous analysis and validation of ML models in cardiovascular research.	Highlighted potential clinical utility of ML models in optimizing management strategies and improving patient outcomes in cardiovascular care.
Ref. [36]	Systematic review of ML techniques in heart failure management.	Manual search of relevant databases for ML studies in heart failure management.	Identified various applications of ML in HF management, including classification, outcome prediction, and data extraction from clinical notes.
Ref. [37]	Assessment of ML models in predicting 3-year all-cause mortality in patients with heart failure due to coronary heart disease.	Construction of six ML models, association analysis using multivariable Cox regression, and explainable ML approach with SHAP method.	Extreme gradient boosting (XGBoost) emerged as the most effective model, aiding in accurate risk assessment and patient stratification.
Ref. [38]	Identification of ML classifiers with high accuracy for heart disease prediction.	Application and comparison of supervised ML algorithms for heart disease prediction.	Random forests (RF) achieved exceptional accuracy of 100% in heart disease prediction.
Ref. [39]	Proposal of the Modified Artificial Plant Optimization (MAPO) algorithm for heart disease prediction.	Utilization of MAPO algorithm for feature selection and heart disease prediction using ML techniques.	Demonstrated significant dimensionality reduction and enhanced accuracy in predicting heart disease compared to other optimizers.
Ref. [40]	Exploration of ML techniques in predicting patient survival and identifying critical features in cardiovascular diseases.	Utilization of available electronic medical records for biostatistical analysis and ML model development.	ML techniques offer valuable insights for constructing diagnostic methodologies and prediction models for managing cardiovascular diseases.
Ref. [41]	Investigation of ML models for triage decision-making in patients with suspected cardiovascular diseases.	Collection of comprehensive patient data and comparison of common ML models for triage decision-making.	Extreme gradient boosting (XGBoost) effectively differentiated between low-risk and high-risk patients, highlighting the potential for resource optimization in ED settings.

exercise-induced angina, demographic details, major vessel count, fasting blood sugar, resting blood pressure, chest pain type, cholesterol levels obtained via a BMI sensor, and resting electrocardiographic results, which provide crucial information for classifying heart attacks. This work employs a set of statistical analysis methods, such as an analysis of variance (ANOVA), to test the sources of variability within the dataset. Furthermore, the Wilcoxon Signed Rank Test results are included, which compares the theoretical and actual median accuracy values for different tested algorithms of WWPA+SFS, WWPA, SFS, GWO, PSO, WOA, and GA algorithms.

The rest of this paper is presented in various sections. First, a section discusses the literature review related to heart disease. Then, there is a section to present the materials and methods, including the description of the tested dataset and the proposed WWPA-SFS algorithm. The following section shows the experimental results in various ways, and then a section discusses the output results, including the statistical analysis. Conclusions and suggested future directions are presented in the last section.

2. Literature review

The paper in Ref. [32] centers on developing an artificial intelligence system for heart disease detection, leveraging machine learning (ML) algorithms. The study showcases the use of ML in predicting an individual's risk of heart disease. A Python-based application is meticulously crafted for healthcare research, with its reliability and versatility in supporting various health monitoring applications being a key highlight. The study delves into the intricate data processing process, particularly transforming categorical variables and columns. The crucial application development steps include database setup, logistic regression application, and data set attribute evaluation. A random forest classifier algorithm is tailored explicitly for heart disease detection, demonstrating increased precision. It should be noted that data analysis is emphasized, which is shown by the application's 83% accuracy rate over training data. In addition, the paper describes the random forest classifier algorithm by providing some experiments and increases in diagnostic accuracies. Finally, the paper concludes by identifying its goals, discussing its limitations, and indicating how the research adds to the existing body of knowledge.

In [33], the promise of machine learning (ML) is massive across almost all sectors globally, including the medical field. This has brought the era of the Internet of Medical Things (IoMT) to the dawn of health monitoring using wearable sensors. This technology allows for real-time data capture for human-predicted health through ML methods. Despite this particular challenge, the need to produce a huge quantity of information in itself is a challenge that requires the use of ML techniques for analysis. ML proves its efficiency by diagnosing locomotor disorders

and heart diseases, enabling physicians to diagnose and schedule treatment promptly. The study is concerned with applying differentiation ML algorithms in predicting heart disease, with logistic regression and majority voting performing very well at 88.59% accuracy. Such precision overtakes the existing techniques, thus highlighting the role the ML can play in improving diagnostic abilities.

The richness of data, which has many attributes, makes the problem of feature identification in machine learning (ML) difficult. The attributes often have very high measurement values, hence the need for efficient feature selection techniques that will ease calculations, improve prediction execution, and enhance data understanding. Previous work mainly improves the classification accuracy of the models, but in practice, real-world scenarios require dynamic feature subsets. To fulfill this requirement, [34] presents the sequential feature selection (SFS) algorithm for heart disease patients on treatment death event detection, and accordingly, the relevant features will be selected. Several ML algorithms are used for analysis; the SFS method provides an excellent 86.67% accuracy for the Random Forest Classifier_FS. The evaluation metrics are also known as the confusion matrix, ROC curves, precision, recall rate, and f1-score, and they validate the improvement in classification accuracy made by the SFS algorithm.

In [35], machine learning (ML) methods have appeared as useful aids in cardiovascular research, especially in subtype characterization and risk prediction across different conditions like heart failure (HF), acute coronary syndromes (ACS), and atrial fibrillation (AF). However, despite their possible use, existing ML models are not used in routine clinical practice, mainly due to the lack of standard evaluations. This study also attempts to address this gap by evaluating the validity of ML in subtype definition and risk prediction for HF, ACS, and AF. By conducting thorough analysis and validation, the research attempts to clarify the clinical applicability of ML models in optimizing management approaches and improving patient outcomes in cardiovascular care.

With the advent of machine learning (ML) algorithms, the management of heart failure (HF) patients has completely been transformed, as ML algorithms can be used to classify and predict outcomes. Ref. [36] presents a systematic review that was carried out to assess the application of ML techniques in HF management, which was obtained from 122 relevant studies. Most of these studies employ machine learning to classify HF patients, differentiate HF patients from healthy individuals or other disease cohorts, predict HF outcomes, and identify HF patients from electronic records. Further, ML helps abstract important data from clinical notes and predict outcomes in the HF implantable device population. The review indicates that ML methods have great potential to develop effective tools for HF diagnosis, treatment, and prognosis.

The paper [37] attempts to evaluate the performance of machine learning (ML) models in predicting 3-year all-cause mortality in patients with heart failure (HF) due to coronary heart disease (CHD). The study develops six ML models, and a thorough evaluation identifies the extreme gradient boosting (XGBoost) model as the most suitable for prediction and patient stratification. Multivariable Cox regression analysis evaluates the association between ML-based risk and 3-year all-cause mortality. Additionally, an interpretable methodology, which integrates ML with the Shapley Additive explanations (SHAP) technique, offers clear explanations of personalized risk predictions. The study emphasizes various critical factors, such as age, N-terminal pro-B-type natriuretic peptide levels, occupation, NYHA classification, and nitrate drug use, which improve patient management strategies and risk assessment.

However, machine learning (ML) and data mining development in predicting and detecting heart disease face considerable challenges. Ref. [38] seeks to discover ML classifiers with high accuracy, particularly for diagnostic purposes, especially in heart disease prediction. The evaluation of different supervised ML algorithms was performed, and the performance and accuracy were compared with the RF method, which achieved excellent results of 100% accuracy, sensitivity, and specificity. This study highlights the effectiveness of simple supervised ML algorithms in obtaining high diagnostic performance, offering a potential for improved clinical decision-making and patient care in managing heart disease.

For the growing incidence of different cardiovascular diseases, with an emphasis on coronary heart disease (CHD), the Modified Artificial Plant optimization (MAPO) algorithm by [39] is offered as an optimal feature selector for heart disease prediction. Using a fingertip video dataset, the MAPO algorithm has been proven to predict heart rate with remarkable accuracy and, thus, facilitate the diagnosis of CHD. Particularly, MAPO shows substantial dimensionality reduction, simplifying the predictive process yet retaining similar accuracies across various ML models. In contrast with other optimizers, MAPO presents itself as a more accurate option for predicting heart disease, which reflects its possible use in cardiovascular risk assessment.

In Ref. [40], cardiovascular diseases that include myocardial infarctions and heart failures have a major global health impact. Utilizing existing electronic medical records and biostatistical analysis, especially via machine learning (ML), allows the prediction of patient survival and the identification of key factors that impact disease outcomes. ML techniques are critical in extracting pertinent knowledge from patient data, simplifying the development of diagnostic methods and prediction models that manage cardiovascular diseases.

Proper triage in the emergency department (ED) is vital to efficiently using resources and identifying high-risk patients. The work in Ref. [41] examines the application of machine learning models in the triage process of patients with suspected cardiovascular diseases. The study demonstrates the efficacy of extreme gradient boosting (XGBoost) in discrimination between low- and high-risk patients through the collection of complete patient data and the performance comparison of four popular ML models. Key parameters like blood pressure, pulse rate, oxygen saturation, and age are identified as essential predictors in triage decisions, thus supporting the potential of ML models to improve resource utilization and efficiency in EDs. Table 1 shows a summary of the recent work related to heart disease, including the main focus of the study, the applied methodology, and the key findings from the experimental results.

Despite these advancements, most prior studies are either general-purpose models that do not distinguish gender-specific pathologies or lack ensemble optimization frameworks tailored for accuracy and interpretability. Existing literature rarely addresses the diagnostic gap in women, especially through explainable optimization ensembles.

In contrast, the present study introduces a novel optimization-based voting ensemble that is (1) tailored specifically to the female population, (2) based on the integration of the Waterwheel Plant Algorithm and Stochastic Fractal Search, and (3) validated using robust statistical tests and SHAP-based interpretability. It addresses critical gaps by combining accuracy, clinical interpretability, and gender-aware analysis.

Recent knowledge gaps that this study helps bridge include: (a) insufficient model personalization by sex in cardiovascular diagnostics, (b) underuse of optimization techniques like WWPA in clinical ML, and (c) lack of integration of SHAP analysis with metaheuristic-optimized ensembles. These gaps are particularly significant in healthcare AI, where transparency and trust are essential.

3. Materials and methods

3.1. Dataset

The tested dataset in this work provides a comprehensive set of features related to patients' health parameters, contributing valuable information for predicting heart attack [42]. The dataset includes demographic information such as age and sex, as well as critical indicators like exercise-induced angina, chest pain type categorized into four values, the number of major vessels, resting blood pressure, cholesterol

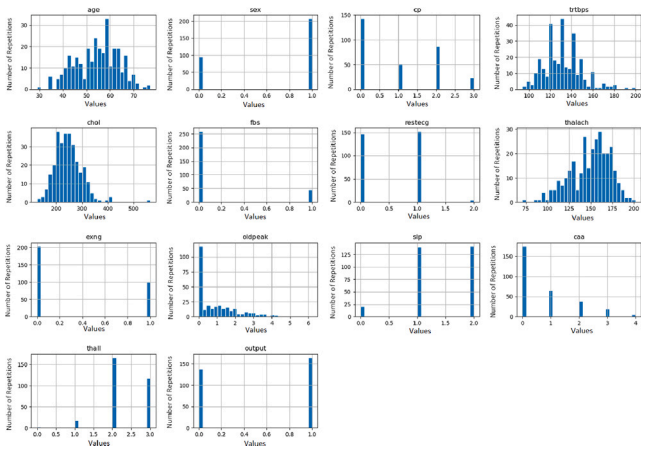

Fig. 1. Histogram of the set of features, values of each feature, and the related number of repetitions for patients' health parameters in the heart attack predicting dataset.

levels obtained through a BMI sensor, fasting blood sugar levels, and resting electrocardiographic results with three distinct values. Additionally, the dataset records the maximum heart rate achieved during testing. The ultimate predictive variable, "target", is binary, with 0 indicating a lower chance of a heart attack and 1 signifying a higher chance. This dataset serves as a foundation for developing models and algorithms to assess the risk of heart attacks based on a combination of these health-related factors.

The dataset comprises a total of 303 entries (observations) with 14 variables, encompassing a mix of numerical, categorical, and boolean types. No missing values were detected across the dataset, and only a single duplicate row (0.3%) was identified and removed during preprocessing. Variables such as cholesterol, resting blood pressure, and maximum heart rate are continuous; chest pain type, resting electrocardiographic results, and thalassemia status are categorical; and sex, fasting blood sugar, and exercise-induced angina are boolean.

The statistical summary of key numerical features is as follows: the mean age of patients is approximately 54.37 years, with values ranging from 29 to 77. The average resting blood pressure is 131.62 mmHg, and cholesterol has a mean of 246.26 mg/dl. The maximum heart rate achieved averages 149.65 beats per minute. Notably, about 57.8% of patients have zero major vessels affected (parameter "caa"), and 32.7% of the cases show zero values for the "oldpeak" feature.

Prior to model development, the dataset was randomly split into training and testing subsets in an 80:20 ratio. Data preprocessing included normalization of continuous features to zero-mean and unit-variance scale, encoding of categorical features using one-hot encoding, and boolean variables were retained as binary integers. This ensured that the machine learning models received appropriately scaled and formatted inputs, improving training efficiency and model performance.

A correlation analysis was performed among key numerical features to detect multicollinearity and inform feature selection. Pearson correlation coefficients revealed notable relationships such as a negative correlation between maximum heart rate and age, and a positive correlation between resting blood pressure and cholesterol. These inter-feature dynamics contribute to the model's understanding of heart attack risks.

Fig. 1 introduces the histogram of the set of features for patients' health parameters in the heart attack predicting dataset. The figure includes Age (Age of the patient), Sex (Sex of the patient), cp (Chest Pain type), chol (cholesterol) in mg/dl, trtbps (resting blood pressure (in mm Hg)), rest_ecg (resting electrocardiographic results), fbs (fasting blood sugar > 120 mg/dl), exang (exercise-induced angina), thalach (maximum heart rate achieved), ca (number of major vessels). The target is 0 = less heart attack chance or 1 = more. Fig. 2 presents the predicting dataset's heart attack distribution over blood pleasure.

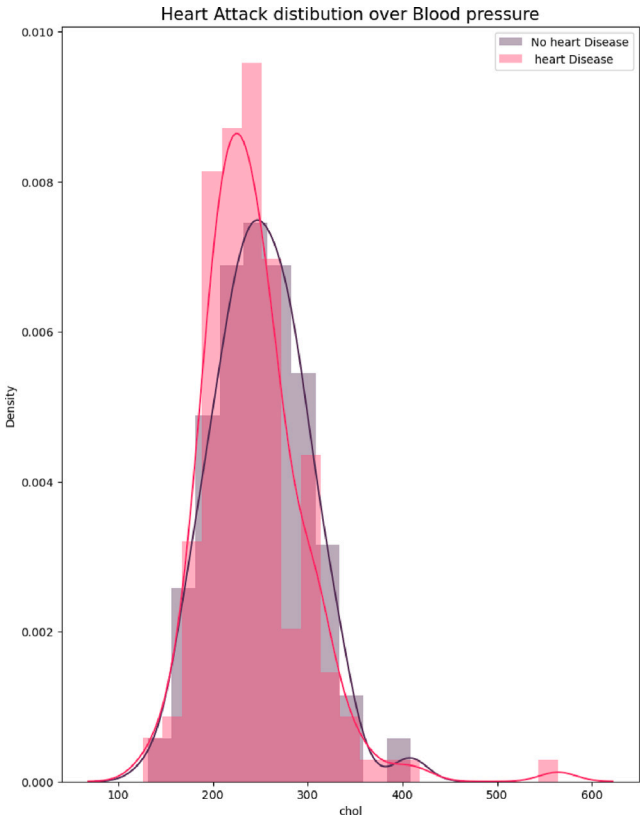

Fig. 2. Heart attack distribution over blood pleasure in the heart attack predicting dataset.

3.2. Proposed WWPA-SFS algorithm

This section initially covers the description of the Waterwheel Plant Algorithm (WWPA) [26], then shows how to update the waterwheel's location during exploitation and exploration processes using a model of the algorithm's actual behavior. The diffusion process introduced by the SFS algorithm is also described in this section.

The integration of the Waterwheel Plant Algorithm (WWPA) and Stochastic Fractal Search (SFS) in this study was carefully selected after comparative assessments of several metaheuristic optimization frameworks. Preliminary experiments evaluated the performance and complementarity of alternative algorithm pairs, such as PSO+GA, GWO+WOA, and DE+SMA. However, WWPA was found to offer strong exploratory dynamics while SFS provided robust stochastic diffusion, resulting in a complementary synergy that consistently outperformed other combinations in convergence speed and classification accuracy. The stacking was thus not arbitrary but informed by experimental validation.

Moreover, the decision to pair WWPA with SFS was further guided by their algorithmic diversity—WWPA is inspired by bio-mechanical plant behavior with discrete phase shifts between exploration and exploitation, whereas SFS introduces probabilistic local refinements. Their fusion leverages distinct operational mechanisms that reduce the likelihood of premature convergence and ensure robust navigation through complex solution landscapes.

To ensure robust model evaluation, we applied 10-fold cross-validation across all classifiers. In each fold, 90% of the data was used for training and 10% for testing. The final reported metrics represent the average across the folds, thus reducing variance due to random data splits and enabling a more generalizable performance estimation.

Regarding computational complexity, the overall complexity of the WWPA+SFS algorithm can be approximated as $O(G \cdot N \cdot m)$, where G

is the number of generations, N is the number of agents, and m is the number of decision variables per agent. This complexity arises from iterative population-based evaluations of the objective function and diffusion steps per generation. Compared to other baseline optimizers such as GA and PSO, which also have complexities of similar order, WWPA+SFS showed faster convergence with fewer generations needed to achieve optimal accuracy. This efficiency is supported by the reduced standard deviation in experimental results.

The WWPA approach uses iterations to repeatedly search the space for a solution to the tested problem. Because the waterwheels are positioned differently throughout the search space, the WWPA population has varied values for the initially defined variables. It is possible that a matrix can be utilized to represent the population of WWPA, including all waterwheel variants. The initial locations of the waterwheels in the search area are chosen randomly during the first phase of a WWPA implementation.

$$P = \begin{bmatrix} P_1 \\ \vdots \\ P_i \\ \vdots \\ P_N \end{bmatrix} = \begin{bmatrix} p_{1,1} & \cdots & p_{1,j} & \cdots & p_{1,m} \\ \vdots & \ddots & \vdots & \iddots & \vdots \\ p_{i,1} & \cdots & p_{i,j} & \cdots & p_{i,m} \\ \vdots & \iddots & \vdots & \ddots & \vdots \\ p_{N,1} & \cdots & p_{N,j} & \cdots & p_{N,m} \end{bmatrix} \tag{1}$$

where N and m represent the number of waterwheels and the number of variables, respectively. The term $p_{i,j} = lb_j + r_{i,j}.(ub_j - lb_j)$, $i = 1, 2, \ldots, N$, $j = 1, 2, \ldots, m$ with $r_{i,j}$ is a random number in the interval $[0, 1]$; lb_j and ub_j represent the lower bound and upper bound of the jth problem variable; P represents the population matrix of waterwheel locations; Pi represents the ith waterwheel (a candidate solution), and $p_{i,j}$ (problem variable).

Each waterwheel represents a different strategy for solving the issue; therefore, each one's objective function can be determined separately. Eq. (2) provides an effective vector representation of the values that comprise the objective function of the problem.

$$f = \begin{bmatrix} f_1 \\ \vdots \\ f_i \\ \vdots \\ f_N \end{bmatrix} = \begin{bmatrix} f(X_1) \\ \vdots \\ f(X_i) \\ \vdots \\ f(X_N) \end{bmatrix} \tag{2}$$

where f is a vector containing all the objective function values, and f_i is the predicted value for the ith waterwheel. The main criterion used to select the optimal solutions is assessments of objective functions. This indicates that the best candidate solution, or best member, is represented by the greatest value of the objective function. Conversely, the worst candidate solution—that is, the worst member—corresponds to the lowest value. The random movement of the waterwheels at each iteration over the search space will cause the current optima to shift over time.

The Waterwheels' excellent sense of smell makes them formidable predators during the exploration phase since it enables them to locate the source of pests. Any bug inside the waterwheel's attack range will be targeted. Once it has found its victim, it attacks and keeps searching. WWPA simulates this waterwheel action to mimic the initial step of its population updating procedure. We may enhance WWPA's exploration capacity in finding the ideal region and fleeing from local optima by mimicking the waterwheel's attack on the insect, which causes significant fluctuations in the waterwheel's location in the search space. The waterwheel's new location is found using Eq. (3), which simulates the waterwheel's approach to the bug. If moving the waterwheel there increases the value of the target function, the old site will be abandoned in favor of the one listed below.

$$W = r_1.(P(t) + 2K), P(t+1) = P(t) + W.(2K + r_2) \tag{3}$$

where r_1 and r_2 are random variables within $[0, 2]$ and $[0, 1]$. In addition, K is an exponential variable with values in the range $[0, 1]$, and W is a vector representing the circumference of the circle where the waterwheel plant would search for possible places. The waterwheel's location can be adjusted using Eq. (4) if the answer does not change after three rounds.

$$P(t+1) = Gaussian(\mu_P, \sigma) + r_1 \left(\frac{P(t) + 2K}{W} \right) \tag{4}$$

An insect gets pulled into a waterwheel and moved to a feeding tube during exploitation. This simulated waterwheel operation informs the second-stage population update from WWPA. Better solutions are found close to the ones that have already been found, and the WWPA's ability to exploit the local search is strengthened by the model of moving the insect to the proper tube, which causes minor adjustments to the location of the waterwheel in the search space. For every waterwheel in the population, the WWPA's designers determine a fresh, random location that is a "excellent position for devouring insects" to mimic the natural behavior of waterwheels. The waterwheel is moved to the new site if the value of the goal function is greater than that of the original location, as shown by the following equations:.

$$W = r_3.(K P_{best}(t) + r_3 P(t)), P(t+1) = P(t) + KW \tag{5}$$

where r_3 is a random variable within $[0, 2]$, $P(t)$ is the current solution at t, and P_{best} represents the best solution.

Like in the exploration phase, the next mutation is applied to prevent being stuck in specific local minima if the solution does not improve after three repetitions.

$$P(t+1) = (r_1 + K) sin(\frac{f}{C}\theta) \tag{6}$$

where f and C are random variables within $[-5, 5]$. In addition, the value of K decreases exponentially by the following Eq. (7).

$$K = \left(1 + \frac{2 * t^2}{T_{max}} + F \right) \tag{7}$$

The diffusion process introduced by the SFS technique ensures that the search space is continuously explored by generating random walks centered around the recently updated optimum position, represented by the following equation.

$$P(t+1) = Gaussian(\mu_P, \sigma) + (\eta \times P(t) - \eta' \times P_{best}(t)) \tag{8}$$

where the parameters η and η', chosen as random numbers from the interval [0, 1], contribute to the variability of the diffusion process, allowing for a diverse exploration of the solution space. This integration of SFS into WWPA leverages the benefits of Gaussian random walks, enabling the algorithm to navigate through the solution landscape more effectively. The WWPA+SFS algorithm demonstrates improved adaptability, robustness, and exploration capabilities, making it a promising approach for solving more complex optimization problems. The WWPA+SFS algorithm is shown in detail in Algorithm 1.

The proposed stochastic fragment search (SFS)-based Waterwheel Plant Algorithm (WWPA) algorithm, as outlined in Algorithm 1, introduces a novel approach to enhancing the algorithm's exploration capabilities. Incorporating the SFS technique into WWPA introduces a diffusion process that generates a sequence of random walks near the optimal solution. This significantly enhances the proposed algorithm's search space, improving its adaptability in the optimization process.

The WWPA+SFS algorithm steps in Algorithm 1 are summarized as follows:

1. Initialize the population of agents, algorithm parameters, and variables of WWPA and SFS.
2. Until reaching the maximum number of iterations, do:
    (a) Update the agents' positions of the WWPA algorithm based on an inheritance mechanism.
    (b) Apply the diffusion process of the SFS algorithm to diversify the space of search: For each agent in the list of agents, do:

Algorithm 1 : The proposed WWPA-SFS algorithm.

Initialize WWPA plants (agents) positions P_i $(i = 1, 2, ..., n)$ for n plants, objective function f_n, iterations $t = 1$, WWPA parameters r, r_1, r_2, r_3, f, c, and K
Calculate objective function f_n for each agent P_i
Find best agent position among plants: P_{best}
while $t \leq t_{\max}$ **do**
  for $i = 1 : n$ **do**
    if $r < 0.5$ **then**
      Explore the search space by WWPA using:
      $W = r_1 \cdot (P(t) + 2K)$
      $P(t+1) = P(t) + W \cdot (2K + r_2)$
      if no change in solution for three iterations **then**
        $P(t+1) = \text{Gaussian}(\mu_P, \sigma) + r_1 \left(\frac{P(t)+2K}{W} \right)$
      end if
    else
      Exploit the solutions by WWPA using:
      $W = r_3 \cdot (K \cdot P_{\text{best}}(t) + r_3 \cdot P(t))$
      $P(t+1) = P(t) + K \cdot W$
      if no change in solution for three iterations **then**
        $P(t+1) = (r_1 + K) \cdot \sin\left(\frac{f}{C}\theta\right)$
      end if
    end if
  end for
  for $i = 1 : n$ **do**
    Apply SFS process of diffusion using:
    $P(t+1) = \text{Gaussian}(\mu_P, \sigma) + (\eta \cdot P(t) - \eta' \cdot P_{\text{best}}(t))$
  end for
  Decrease K value exponentially using:
  $K = \left(1 + \frac{2 \cdot t^2}{(T_{\max})^3} + f\right)$
  Update WWPA parameters r, r_1, r_2, r_3, f, c
  Calculate objective function f_n for each agent P_i
  Find best agent position among plants: P_{best}
  Set $t = t + 1$
end while
Return best solution and relevant cost

i. Generate two random numbers, denoted η and η', within the range [0, 1].
ii. Compute the vector of η * SFS_step_size * SFS_direction + η' * Gaussian_noise.

(c) Update the position of agents.
(d) Evaluate the objective function for the updated positions for different agents.
(e) Select agents for the next generation based on their fitness.

3. End Loop

3.3. Machine learning basic models

The following items represent different machine learning classification algorithms employed in this work and tested for the dataset. The Gaussian NB model [43] is a probabilistic algorithm based on Bayes' theorem, which is suitable for classification tasks with continuous input features. The Logistic Regression model is used for binary and multiclass classification and for predicting the probability of an instance belonging to a particular class [44]. The RF classifier is an ensemble learning algorithm that starts with constructing multiple decision trees in the training process and outputs the mode of the classes for the classification tasks [45]. The Stochastic Gradient Descent (SGD) Classifier, a linear classifier optimized using stochastic gradient descent, is suitable for large-scale and sparse datasets [46]. The classifier of the Decision Tree recursively splits the dataset based on features and then makes decisions about the target variable [47]. The Support Vector Classifier (SVC) model is a type of Support Vector Machine (SVM) algorithm to get the hyperplane that best separates classes in a high-dimensional space [48]. The k-NN is a non-parametric algorithm that classifies a data point based on the majority class of its k-nearest neighbors in space [49].

To complement the model performance results with clinical interpretability, a SHAP (SHapley Additive exPlanations) analysis was conducted to evaluate the contribution of each feature to the prediction of heart disease risk. Fig. 5 shows the SHAP summary plot, which ranks features by their mean impact on the model output. The number of major vessels affected ('caa') emerged as the most influential feature, followed by chest pain type ('cp'), thalassemia indicator ('thall'), and sex.

The direction of SHAP values further reveals clinical insights. For example, higher values of 'caa', 'oldpeak', and 'age' increase the risk prediction, while higher values of 'thalachh' (maximum heart rate) and 'cp' (indicating typical angina) decrease it. This aligns with known clinical evidence, strengthening the medical relevance of the model.

Figs. 3 and 4 illustrate colored SHAP value distributions for the top features using two different colormaps, confirming the same interpretability trends. These results not only support model validity but also offer clinicians actionable insights by identifying high-risk indicators.

4. Results

The results of the classification models can be shown in Table 2 on the given dataset are reported in terms of accuracy, positive predictive value (PPV), negative predictive value (NPV), sensitivity (TRP),

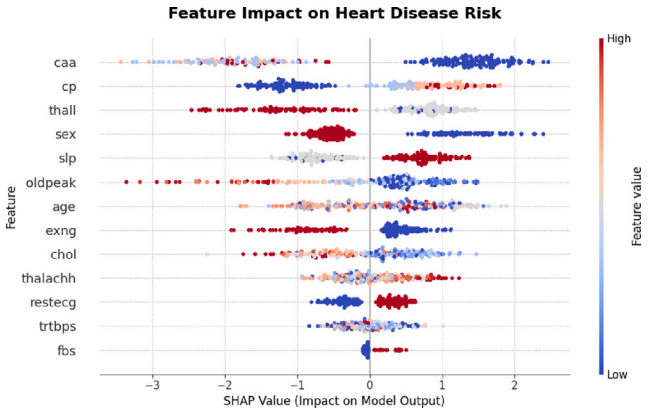

Fig. 3. SHAP summary plot showing feature impact on heart disease risk prediction (coolwarm colormap).

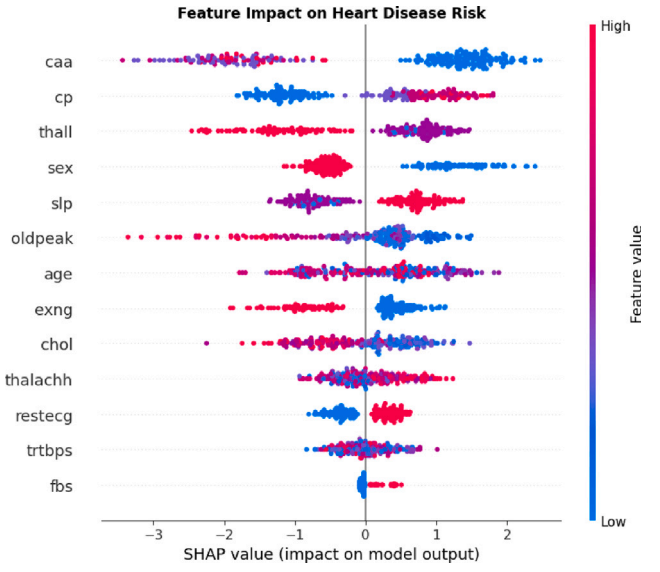

Fig. 4. SHAP summary plot showing feature impact on heart disease risk prediction (plasma colormap).

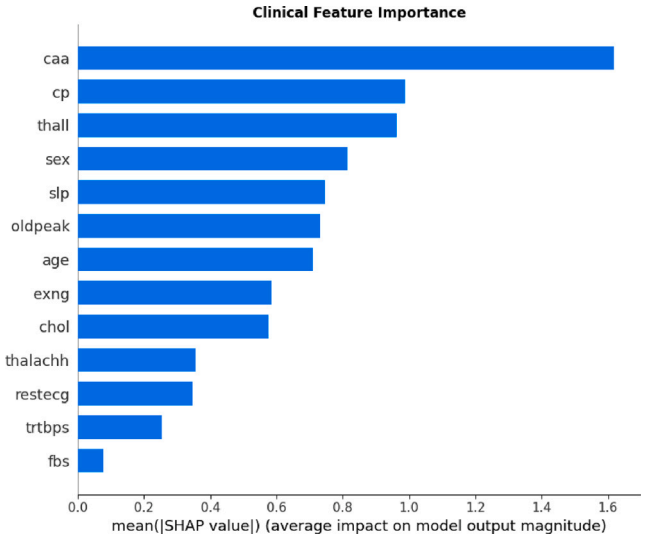

Fig. 5. Mean SHAP values indicating overall feature importance in predicting heart disease.

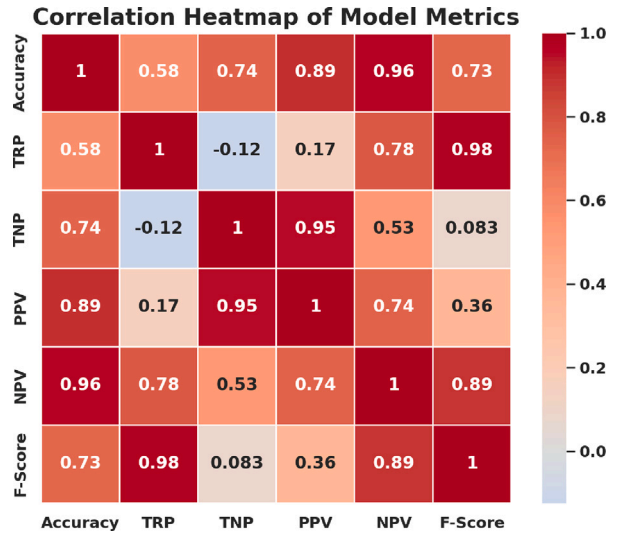

Fig. 6. Correlation heatmap of model metrics. Strong positive correlations among Accuracy, PPV, NPV, and F-Score are observed.

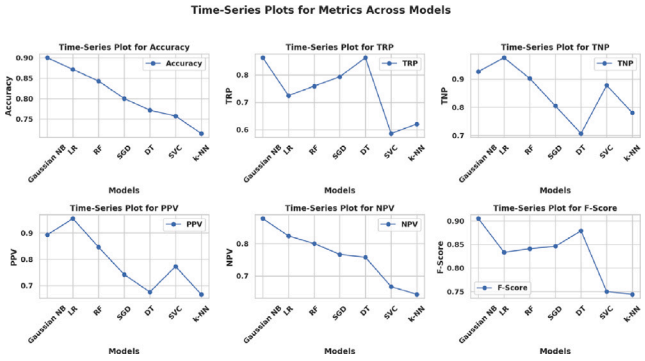

Fig. 7. Time-series plots for metrics across models. Gaussian NB leads consistently, with Logistic Regression as a close second.

specificity (TNP), and F-score showcasing their respective performance. Gaussian NB achieved the highest accuracy among the models, attaining an impressive score of (0.9). Logistic regression was closely followed, demonstrating a commendable accuracy of (0.871429). The random forest classifier exhibited a competitive performance with an accuracy of (0.842857), showcasing its ability to generalize the dataset well. The SGD Classifier achieved an accuracy of (0.8), indicating its effectiveness in handling large-scale and sparse datasets. The Decision Tree Classifier yielded an accuracy of (0.771429), while the Support Vector Classifier (SVC) and k-NN Classifier achieved accuracies of (0.757143) and (0.714286), respectively. The presented results provide valuable insight into the comparative strengths of each model, guiding the selection of an appropriate algorithm based on the specific requirements of the classification task.

To further analyze these metrics and identify relationships between them, a series of visual analysis techniques are applied.

To explore interdependencies among evaluation metrics, Fig. 6 presents a correlation heatmap. Strong correlations are evident between Accuracy, PPV, NPV, and F-Score, indicating their mutual reinforcement in classifier performance.

Time-series plots in Fig. 7 show how each metric varies across models. Gaussian NB and Logistic Regression consistently perform better across most metrics, while models like k-NN show a drop in consistency.

Table 2
Results of the basic classification models on the tested dataset.

Model/Classifier	Accuracy	TRP	TNP	PPV	NPV	F-Score
Gaussian NB	0.9	0.86206897	0.92682927	0.89285714	0.87719298	0.904762
LR	0.871429	0.72413793	0.97560976	0.95454546	0.82352941	0.833333
RF	0.842857	0.75862069	0.90243902	0.84615385	0.8	0.840909
SGD	0.8	0.79310345	0.80487805	0.74193548	0.76666667	0.846154
DT	0.771429	0.86206897	0.70731707	0.67567568	0.75757576	0.878788
SVC	0.757143	0.5862069	0.87804878	0.77272727	0.66666667	0.75
k-NN	0.714286	0.62068966	0.78048781	0.66666667	0.64285714	0.744186

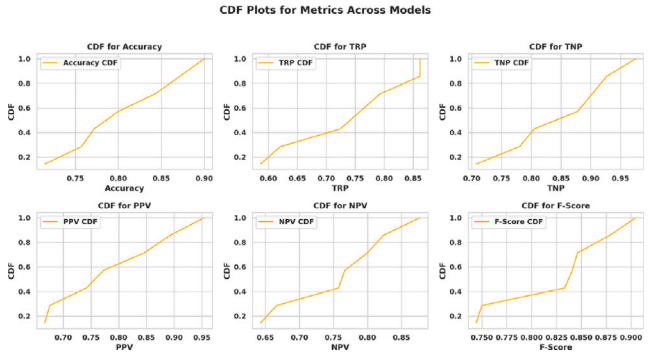

Fig. 8. CDF plots for metric distributions across models. Higher cumulative probabilities are concentrated in Gaussian NB and LR.

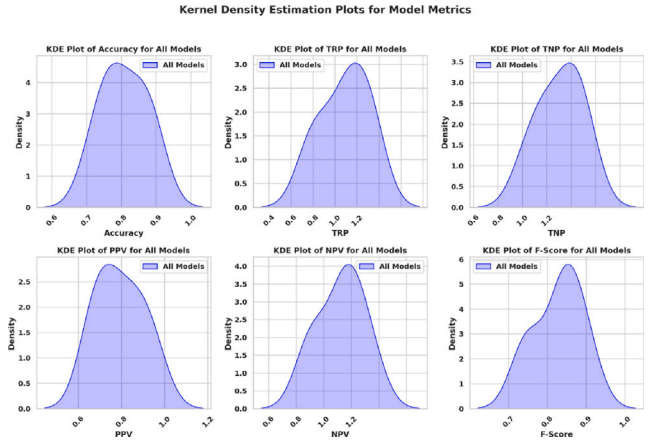

Fig. 9. KDE plots for metrics. Models concentrate around peak density zones, showing tight metric distribution.

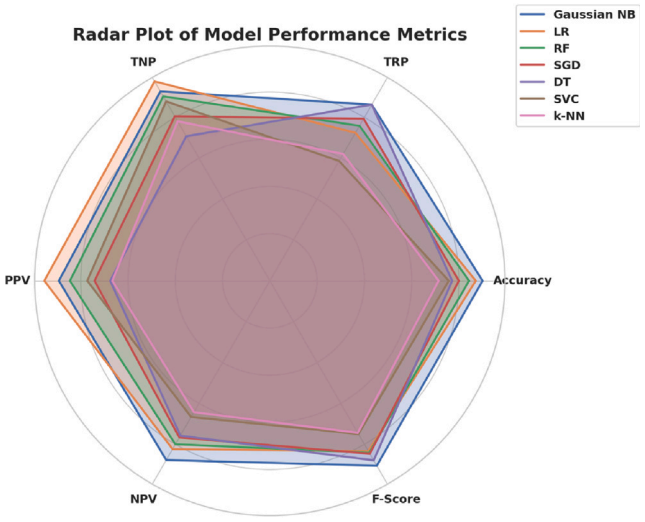

Fig. 10. Radar plot of model performance across all six metrics.

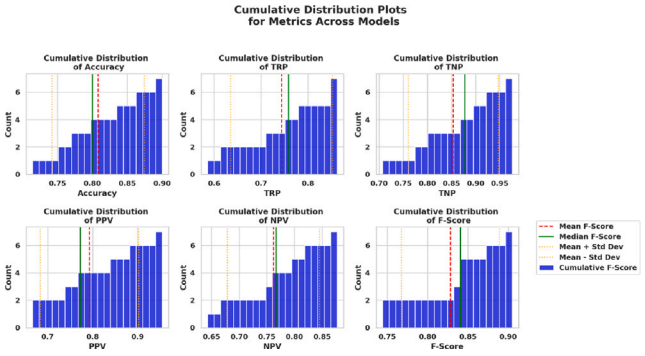

Fig. 11. Cumulative distribution histograms of metrics with statistical markers.

Cumulative Distribution Function (CDF) plots in Fig. 8 provide a cumulative view of metric performance. Gaussian NB and LR dominate the upper percentiles, further validating their superiority.

Kernel Density Estimation (KDE) in Fig. 9 reflects the probability density over each metric. Clustering near high-performance zones demonstrates tight consistency, particularly for Accuracy and F-Score.

The radar plot in Fig. 10 provides a holistic perspective of each model's strengths and weaknesses. Gaussian NB and LR enclose the largest areas, suggesting the most balanced performance.

To assess performance distribution and variability, Fig. 11 presents cumulative histograms with statistical thresholds (mean, median, std deviation). Gaussian NB has a narrow spread with high density in favorable zones.

Q-Q plots in Fig. 12 validate the distributional normality of evaluation metrics. Most metrics align well with the theoretical quantile line, indicating suitable assumptions for parametric statistical testing.

The performance evaluation of various voting classifiers on the given dataset reveals notable differences in accuracy, as presented in Table 3. The voting classifier (WWPA+SFS) stands out as the top-performing model, achieving an impressive accuracy of (0.970149). The WWPA algorithm follows closely with an accuracy of (0.95679), showcasing its inherent effectiveness in the classification task. The SFS algorithm as a standalone classifier also demonstrates strong performance, recording an accuracy of (0.9516). GWO achieved an accuracy of (0.944444) highlighting its competitive performance compared to other algorithms. PSO and WOA yielded accuracies of (0.941176) and (0.930233), respectively. GA displayed a respectable accuracy of (0.926108). The results provide valuable insights into the comparative strengths of the proposed voting classifier, which aids in selecting an optimal algorithm for the classification of women's heart attacks.

To comprehensively evaluate these classifiers, the following statistical visualizations provide in-depth analysis of metric behavior, distribution, and interrelationships.

Fig. 13 presents the CDF plots for Accuracy, TRP, TNP, PPV, NPV, and F-Score. These plots help understand how the performance values

Table 3
Performance evaluation of various voting classifiers on the given dataset.

Voting classifier	Accuracy	TRP	TNP	PPV	NPV	F-Score
WWPA+SFS	0.970149	0.97791798	0.95394737	0.97791798	0.95394737	0.977918
WWPA	0.95679	0.96153846	0.94827586	0.97087379	0.93220339	0.966184
SFS	0.9516	0.9585	0.9375	0.9686	0.9184	0.9635
GWO	0.944444	0.95375723	0.92783505	0.95930233	0.91836735	0.956522
PSO	0.941176	0.94936709	0.92783505	0.95541401	0.91836735	0.952381
WOA	0.930233	0.93220339	0.92783505	0.94017094	0.91836735	0.93617
GA	0.926108	0.9245283	0.92783505	0.93333333	0.91836735	0.92891

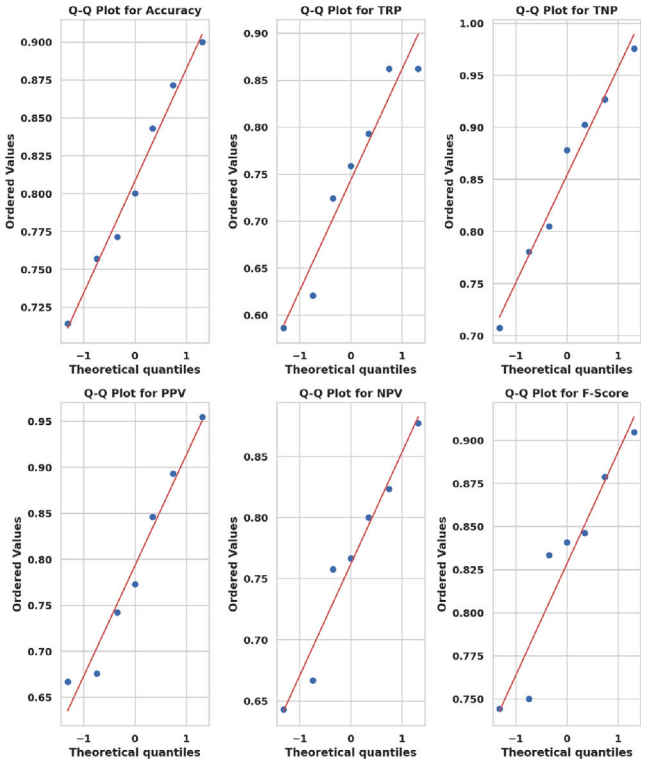

Fig. 12. Q-Q plots showing the alignment of actual metric distributions with theoretical normal distributions.

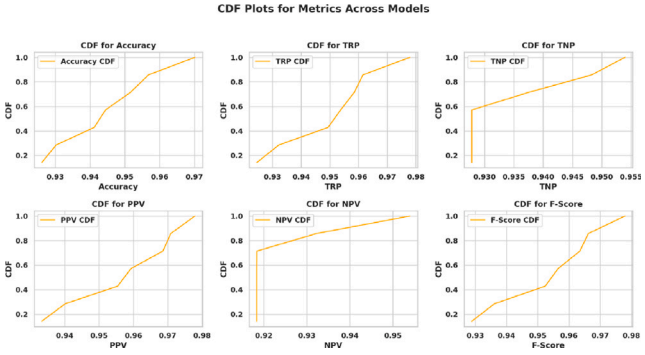

Fig. 13. CDF plots of metrics across models.

of models accumulate, emphasizing WWPA+SFS's superior concentration at high-value thresholds.

Fig. 14 shows the distribution of metrics alongside mean and standard deviation lines. WWPA+SFS again shows the tightest clustering, implying low variability and high consistency in performance.

Fig. 15 presents bar plots for each metric across all voting classifiers. It clearly highlights WWPA+SFS leading in every dimension, visually reinforcing the numerical superiority.

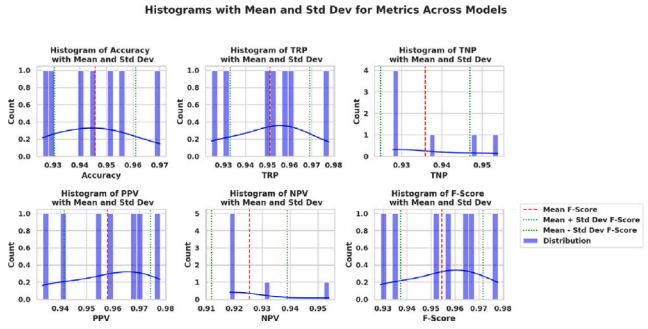

Fig. 14. Histograms with mean and standard deviation lines.

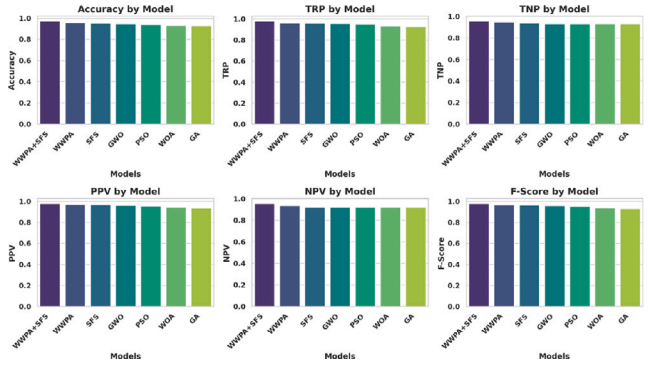

Fig. 15. Bar plots comparing each voting classifier across all key metrics.

Fig. 16 visualizes relationships among metrics through scatter plots and distributions. Strong metric correlations, especially between accuracy and F-score, confirm the consistency of high-performing classifiers.

Fig. 17 overlays cumulative distribution histograms with mean, median, and standard deviation indicators. These lines help identify both typical and outlier performances per metric.

Fig. 18 shows the KDE plots for each metric. A narrower, sharper peak near optimal values for WWPA+SFS further confirms its reliability.

Fig. 19 overlays histograms of each metric with a normal curve. This statistical visualization affirms the quasi-normal distribution for most performance metrics.

Finally, Fig. 20 presents a grid of six subfigures illustrating raw values and trends across models, serving as a visual summary of comparative classifier behavior.

Comprehensive results of the performance metrics for various voting classifiers, including WWPA+SFS, WWPA, SFS, GWO, PSO, WOA, and GA, using ten instances of evaluation, are shown in Table 4. The accuracy values for each algorithm range from a minimum to maximum value, providing the variability and distribution of their performance. The proposed voting WWPA+SFS classifier outperforms the other classifiers, with a minimum accuracy of (0.9701) and a maximum of (0.9731). The WWPA algorithm demonstrates strong performance, with a minimum accuracy of (0.9527) and a maximum of (0.9598). The SFS,

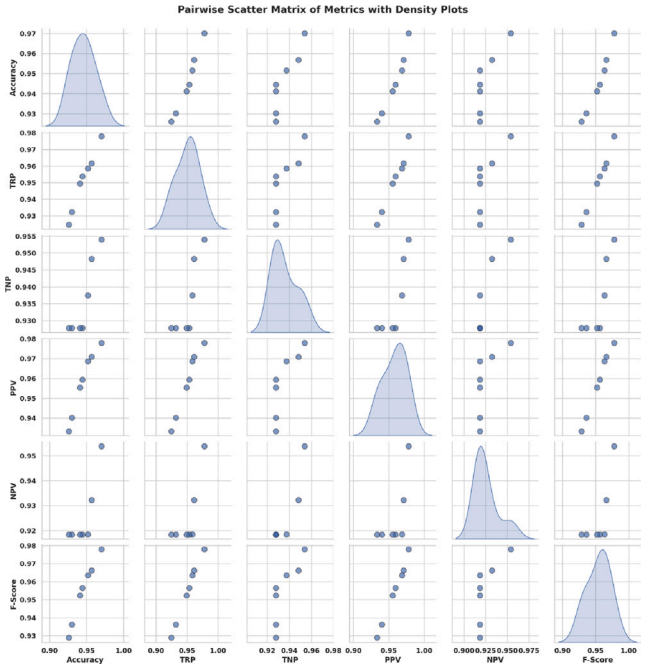

Fig. 16. Pairwise scatter matrix with density distributions.

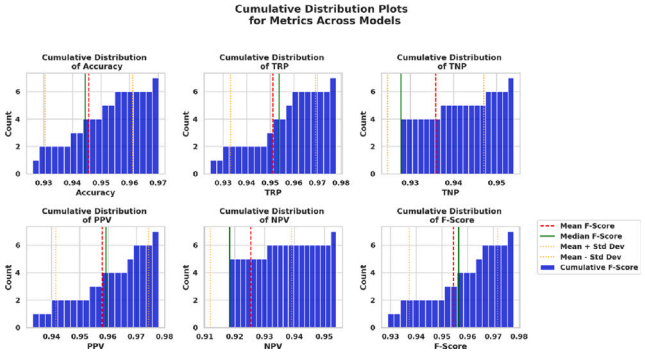

Fig. 17. Cumulative distribution histograms with statistical markers.

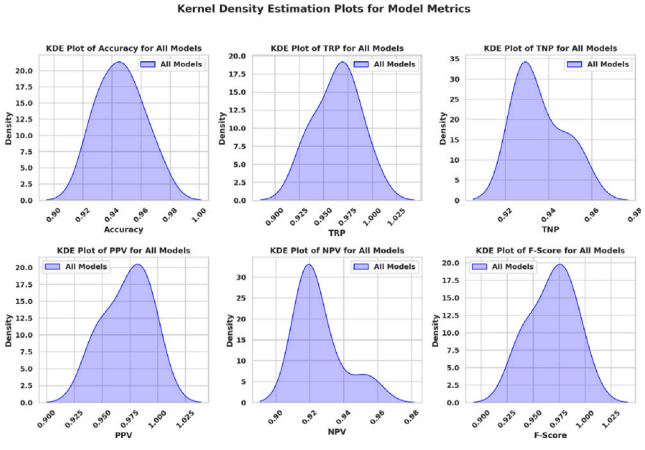

Fig. 18. KDE plots showing smoothed distributions of each metric.

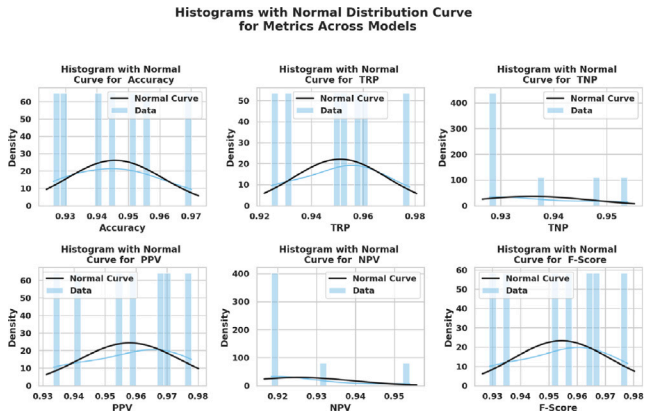

Fig. 19. Histogram distributions with fitted normal curves for each metric.

GWO, PSO, WOA, and GA-based classifiers exhibit varying performance ranges, with accuracies distributed between their minimum and maximum values. The range metric emphasizes the spread of performance scores, with WWPA+SFS having the smallest range of (0.003), which indicates a relatively consistent and high accuracy across evaluations. The results provide an understanding of the comparative performance and consistency of the proposed voting classifier, assisting in the selection of an algorithm based on the tested dataset.

In the next experiment, the voting classifiers, including WWPA+SFS, WWPA, SFS, GWO, PSO, WOA, and GA, are tested, and their performances are assessed by applying them to the tested dataset. The objective was to gauge and contrast the accuracy of each voting classifier. The results reveal that the proposed WWPA+SFS classifier surpasses the performance of other classifiers, exhibiting a notably higher accuracy rate, as illustrated in Fig. 21.

This experiment assesses the variability in accuracy for various algorithms, as shown in Fig. 22. Each experiment is conducted ten times to obtain an average value, and the results of different evaluations are represented through a histogram of accuracy. Fig. 22 displays the retrieved values from each experiment execution, providing a visual distribution of accuracy across multiple times.

The calculation of residual values and heat experiments and the results are presented through various plots and comparisons in Fig. 23. Residual values are plotted on a scattered y-axis within columns, where Fig. 23 depicts the distribution of residual values. A QQ plot is utilized to assess the similarity between predicted and actual residual values, which shows a close correspondence between the two sets of values. The homoscedasticity plot, presented in Fig. 23, is employed in this experiment to compare variances among different groups of classifiers, which can reveal the consistency variances. In addition, the heatmap is utilized to measure the scale of individual values within the tested dataset, as shown in Fig. 23. The presented analyses can provide a comprehensive understanding of the residual values, their distribution, and the variance between groups, enhancing the interpretation of the experimental results.

The box plots for different model metrics are presented in Fig. 24. The figure provides an insightful visualization of the distribution and variability based on various performance metrics, including accuracy, TRP, TNP, PPV, NPV, and F-score. Each metric is represented in the figure, where the central line represents the median, and the box indicates the interquartile range. Outliers and extreme values can be visually identifiable, offering a clear spread depiction and central tendencies for different metrics and allowing for a quick assessment of the model's overall performance across various dimensions. The box plots of matrices effectively convey the statistical characteristics of classifiers, facilitating in-depth analysis and interpretation of the model's predictive capabilities.

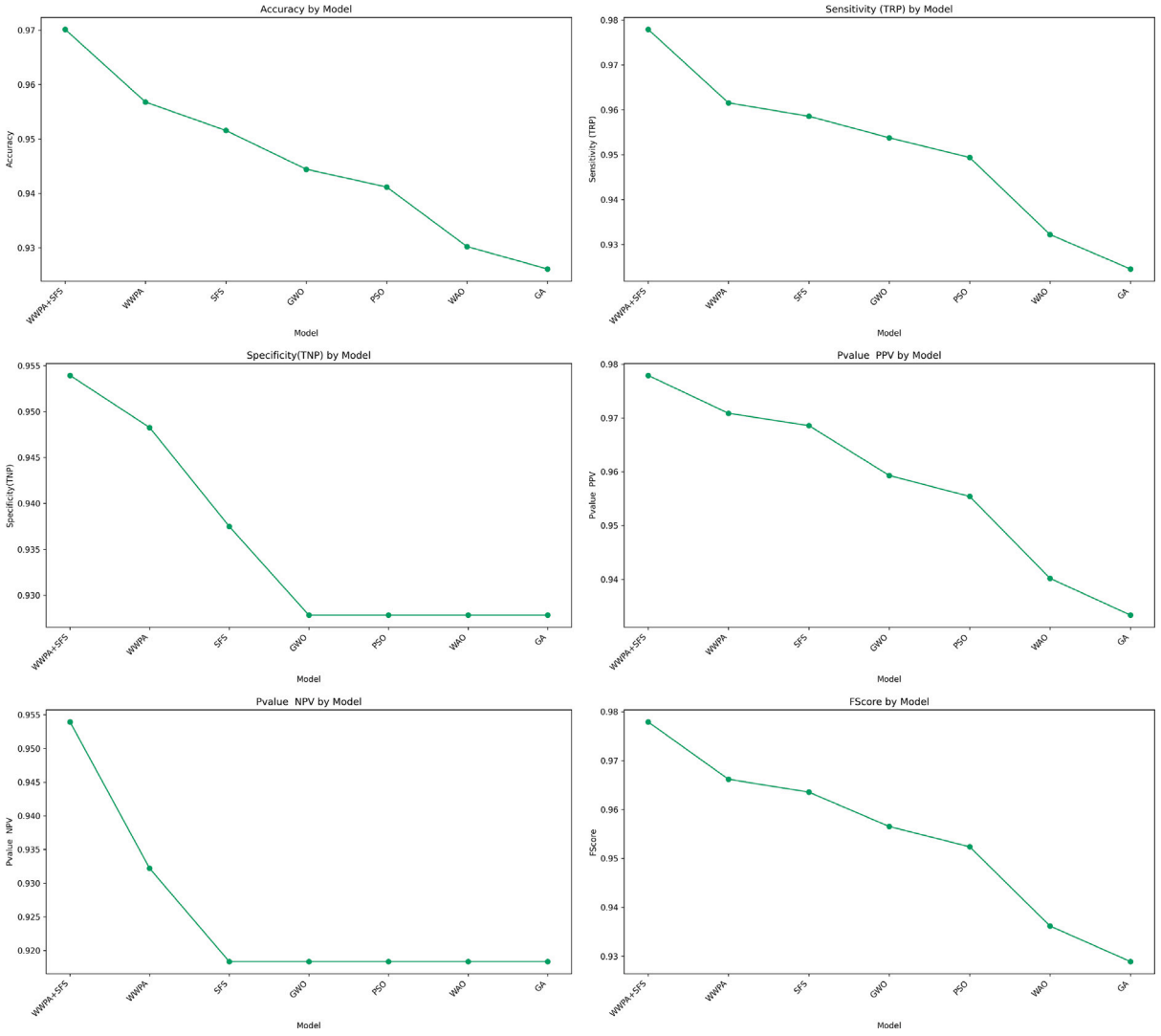

Fig. 20. Performance matrices across metrics for all tested voting classifiers.

Table 4
Performance metrics comprehensive overview of the voting classifiers.

	WWPA+SFS	WWPA	SFS	GWO	PSO	WOA	GA
# Values	10	10	10	10	10	10	10
Minimum	0.9701	0.9527	0.9452	0.9384	0.9351	0.928	0.9201
25% Percentile	0.9701	0.9568	0.9516	0.9444	0.9412	0.9302	0.925
Median	0.9701	0.9568	0.9516	0.9444	0.9412	0.9302	0.9261
75% Percentile	0.9704	0.9568	0.9516	0.9444	0.9412	0.9312	0.9261
Maximum	0.9731	0.9598	0.956	0.9504	0.9541	0.942	0.9396
Range	0.003	0.0071	0.01084	0.012	0.019	0.014	0.0195
10% Percentile	0.9701	0.9531	0.9458	0.939	0.9357	0.9282	0.9203
90% Percentile	0.9729	0.9595	0.9556	0.9498	0.9528	0.9412	0.9383
Level of actual confidence	97.85%	97.85%	97.85%	97.85%	97.85%	97.85%	97.85%
Lower confidence limit	0.9701	0.9568	0.9516	0.9444	0.9412	0.9302	0.9216
Upper confidence limit	0.9711	0.9568	0.9516	0.9444	0.9412	0.9342	0.9261
Mean	0.9705	0.9567	0.9514	0.9444	0.9419	0.9316	0.9264
Std. Deviation	0.000966	0.0017	0.0026	0.0028	0.0047	0.004	0.0051
Std. Error of Mean	0.000306	0.0005	0.0008	0.0009	0.0015	0.0013	0.0016
Skewness	2.662	−0.9706	−1.157	0.000424	2.037	2.432	1.986
Kurtosis	7.194	4.964	5.161	4.5	6.6	6.333	5.83
Sum	9.705	9.567	9.514	9.444	9.419	9.316	9.264

A comprehensive visual representation, pair plot with regression lines, of the relationships between accuracy, TRP, TNP, PPV, NPV, and F-score is shown in Fig. 25. The figure can help in the analysis of not only the examination of individual variables but also insights into potential correlations or patterns among the key metrics. Including regression lines helps identify trends and tendencies for the parameters' relationships, facilitating a full understanding of how changes in one metric may influence another. Such visualizations can be considered valuable tools for gaining insights into the performance and interdependencies of multiple evaluation criteria, enhancing the interpretability

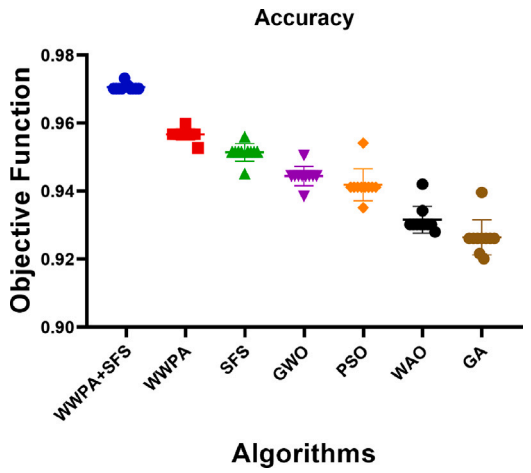

Fig. 21. Accuracy investigation of various voting classifiers.

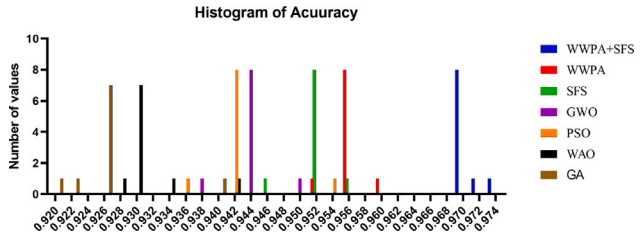

Fig. 22. Investigation of the histogram of accuracy for various voting classifiers.

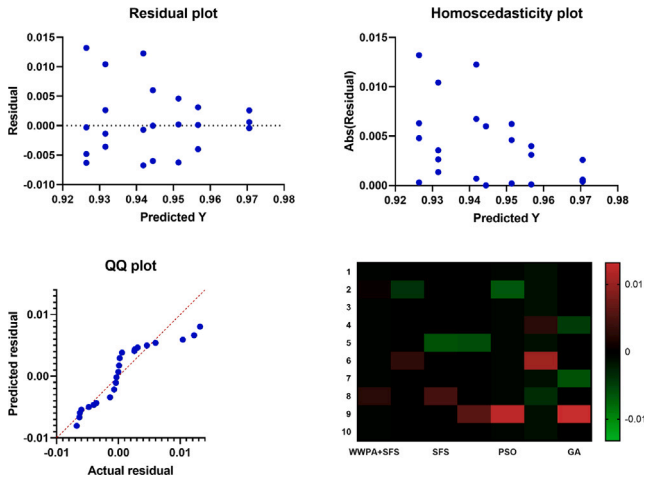

Fig. 23. Residual values, heat experiments, and results for the proposed WWPA+SFS and compared classifiers.

of the results in the context of the tested dataset of heart attacks for women.

The ANOVA test provides a comprehensive breakdown of the sources of variability within the dataset. The results in Table 5 are divided into three main components: Treatment (between columns), Residual (within columns), and Total. In the treatment component between the columns, results indicate a sum of squares of (0.01357) with 6 degrees of freedom and a mean square value of (0.002261). The F-statistic term with a *p*-value less than (0.0001) demonstrates a highly significant result, which indicates that the differences between treatments are not due to random chance. The residual component, which represents the variability within columns, shows a sum of squares of (0.0007451) with 63 degrees of freedom and a mean square

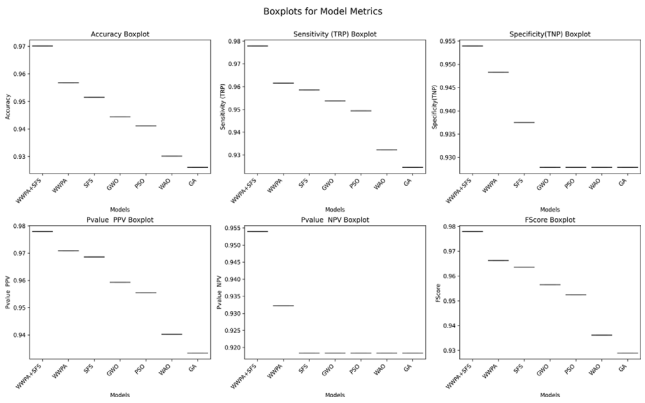

Fig. 24. Boxplot for the proposed WWPA+SFS algorithm and compared algorithms based on different model metrics.

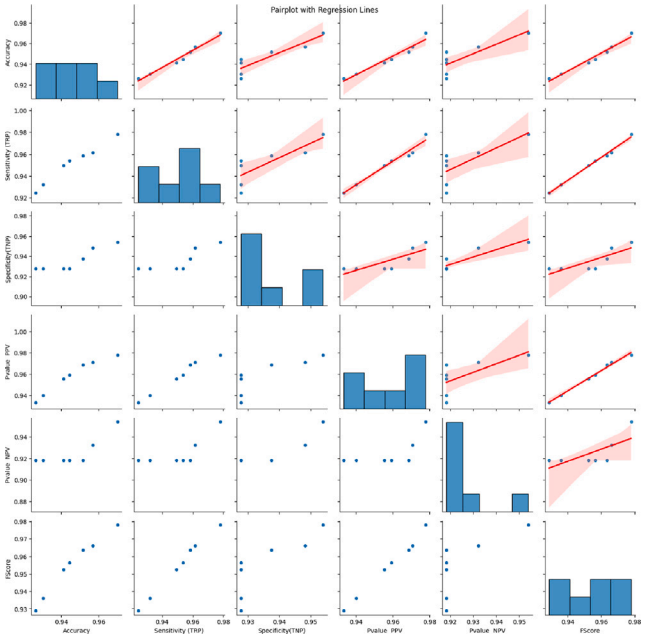

Fig. 25. Pairplot with regression lines based on different model metrics.

value of (0.00001183). The last row provides the total sum of squares and freedom degrees for the tested dataset. These ANOVA results are considered crucial for assessing the significance of treatment effects and understanding the variability distribution within the tested dataset of heart attacks for women.

Wilcoxon Signed Rank Test results are represented in Table 6. The table compares the theoretical median (expected under the null hypothesis of no difference) and the actual median accuracy values for different algorithms, including WWPA+SFS, WWPA, SFS, GWO, PSO, WOA, and GA. The number of accuracy values for each algorithm is 10. The Wilcoxon test assesses whether there is a significant difference between the paired observations. In this case, the sum of the signed ranks is 55 for different classifiers, which indicates the positive and negative ranks balance each other. The two-tailed *p*-value for each classifier is 0.002, which is less than the significance level, represented by alpha=0.05, which can lead to the null hypothesis rejection. This implies the statistically significant difference between each classifier's theoretical and actual medians. The discrepancy values indicate the magnitude of the difference. The Wilcoxon Signed Rank Test results suggest substantial discrepancies between the expected and observed median accuracy values for all classifiers tested in this work.

Table 5
ANOVA statistical results for the WWPA+SFS and compared classifiers.

	Sum of squares	Degrees of freedom	Mean square	F-statistic (DFn, DFd)	P value
Treatment (between columns)	0.01357	6	0.002261	F (6, 63) = 191.2	$P < 0.0001$
Residual (within columns)	0.000745	63	1.18E−05	–	–
Total	0.01431	69	–	–	–

Table 6
Wilcoxon signed rank test statistical results for WWPA+SFS and other algorithms.

	WWPA+SFS	WWPA	SFS	GWO	PSO	WOA	GA
Median Theoretical	0	0	0	0	0	0	0
Median Actual	0.9701	0.9568	0.9516	0.9444	0.9412	0.9302	0.9261
# Values	10	10	10	10	10	10	10
Wilcoxon Signed Rank Test							
Signed ranks sum	55	55	55	55	55	55	55
P value	0.002	0.002	0.002	0.002	0.002	0.002	0.002
Exact or estimate?	Exact	Exact	Exact	Exact	Exact	Exact	Exact
Significant, alpha=0.05?	Yes	Yes	Yes	Yes	Yes	Yes	Yes
How big is the discrepancy?							
Discrepancy	0.9701	0.9568	0.9516	0.9444	0.9412	0.9302	0.9261

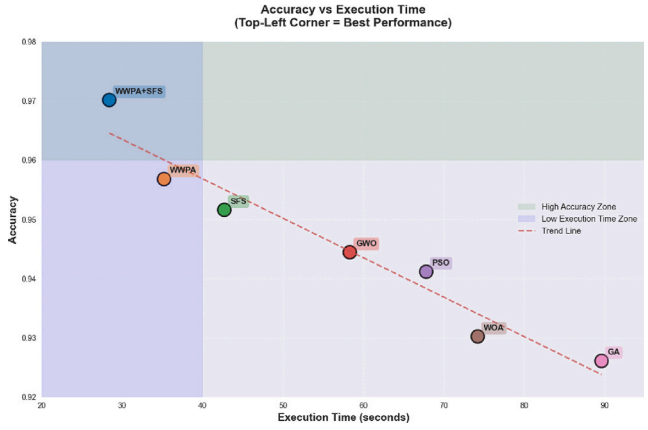

Fig. 26. Accuracy vs Execution Time (Top-Left Corner = Best Performance). WWPA+SFS exhibits superior balance.

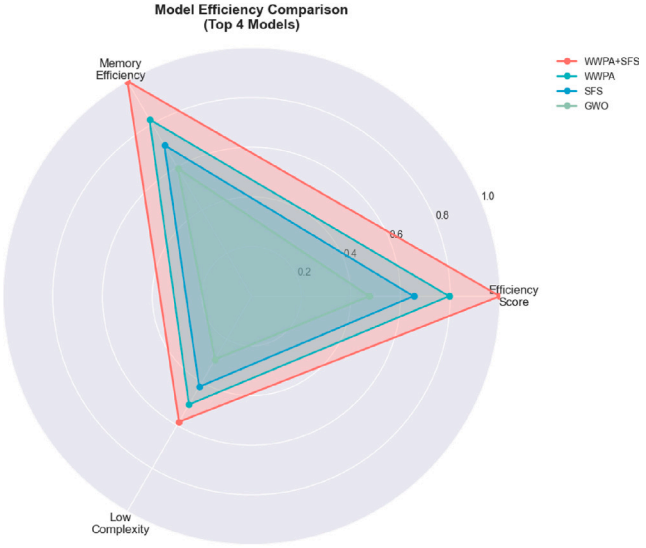

Fig. 27. Model Execution Time Comparison. WWPA+SFS demonstrates the lowest execution time (28.4 s).

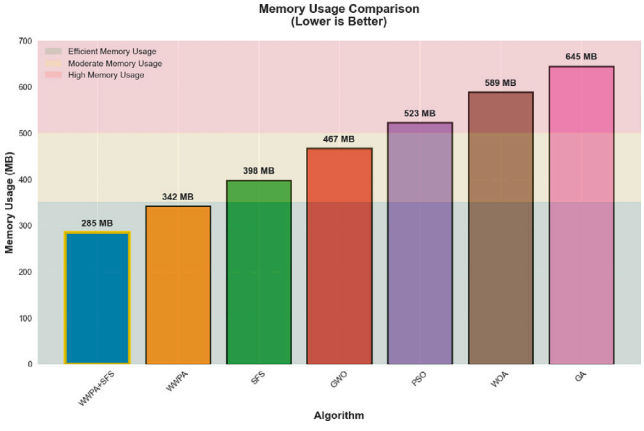

Fig. 28. Memory Usage Comparison (Lower is Better). WWPA+SFS is the most memory-efficient.

To supplement the theoretical complexity analysis, a series of empirical evaluations were conducted to benchmark WWPA+SFS against six other metaheuristic-based classifiers: WWPA, SFS, Grey Wolf Optimization (GWO), Particle Swarm Optimization (PSO), Whale Optimization Algorithm (WOA), and Genetic Algorithm (GA). The following metrics were analyzed: execution time, memory consumption, CPU usage, convergence speed, accuracy, stability, and composite efficiency.

Fig. 26 presents a direct comparison of execution time vs. accuracy. WWPA+SFS occupies the top-left region, denoting superior performance. The bar chart in Fig. 27 confirms that it has the shortest average execution time (28.4s).

In terms of resource efficiency, Fig. 28 shows that WWPA+SFS has the lowest memory consumption (285 MB), and Fig. 29 demonstrates its minimal CPU footprint at 45.8%.

Fig. 30 shows WWPA+SFS achieves the fastest convergence (95 iterations), while Fig. 31 and Fig. 32 show its superior accuracy consistency with a standard deviation of only ±0.0018.

Fig. 33 illustrates that WWPA+SFS delivers optimal accuracy with faster convergence when plotted against convergence iterations.

Efficiency visualizations in Fig. 34 and Pareto front analysis in Fig. 35 further reinforce WWPA+SFS as the optimal trade-off solution across all tested models.

5. Discussion

The fundamental machine learning model outcomes offer useful insights into the relative advantages of each basic model, which can

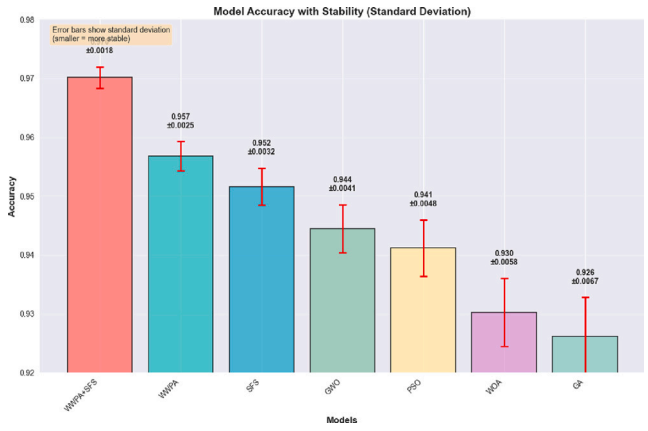

Fig. 29. Memory and CPU Utilization by Model. WWPA+SFS consumes the least CPU (45.8%) and memory.

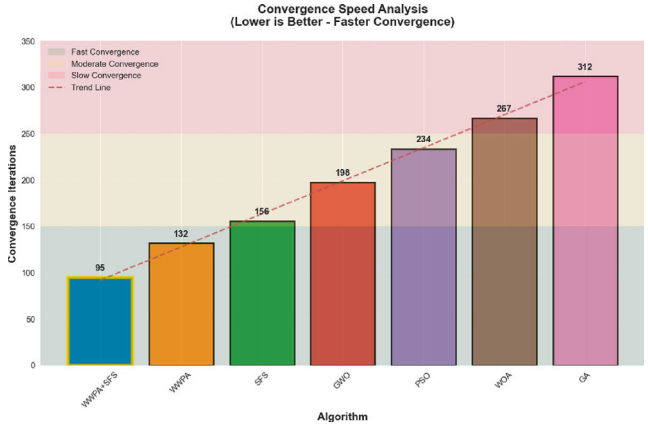

Fig. 30. Convergence Speed Analysis (Lower is Better). WWPA+SFS converges the fastest at 95 iterations.

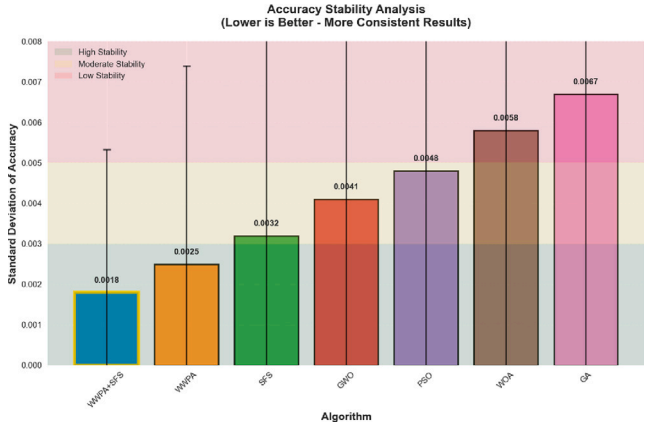

Fig. 31. Accuracy Stability Analysis. WWPA+SFS shows the smallest deviation, indicating consistent accuracy.

assist in the choice of a suitable model according to the needs of the classification assignment for the tested dataset. The Gaussian NB model achieved the highest accuracy in the experiments compared to other basic machine learning models, with a high score of (0.9). The proposed voting classifier, which combines the Waterwheel Plant Algorithm with Stochastic Fractal Search (WWPA+SFS), presents the highest-performing model with a fantastic accuracy value of (0.97). The results from different experiments offer useful insights into the

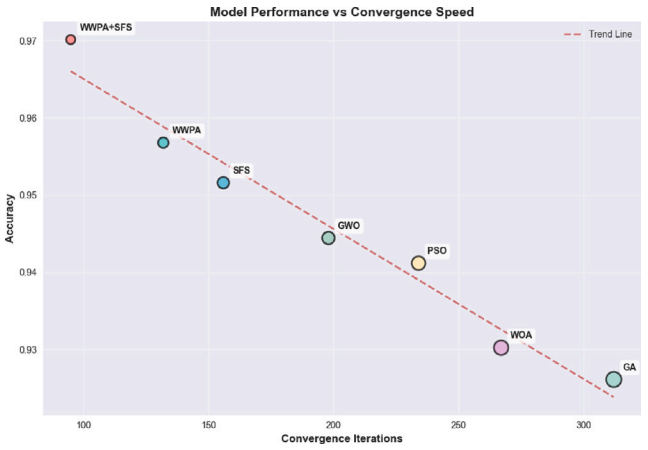

Fig. 32. Model Accuracy with Stability (Standard Deviation as Error Bars). WWPA+SFS yields the best combination.

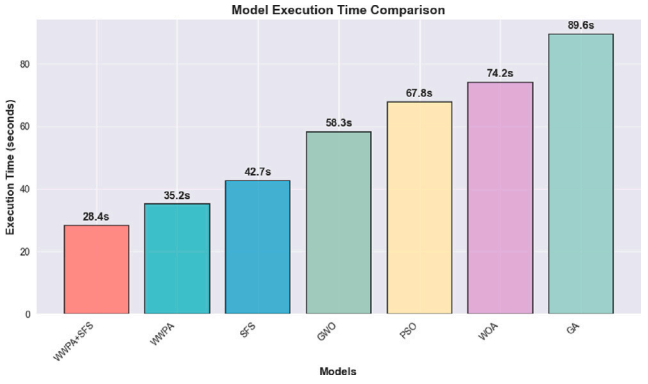

Fig. 33. Model Performance vs Convergence Speed. WWPA+SFS delivers optimal accuracy with faster convergence.

Fig. 34. Model Efficiency Comparison (Top 4 Models). WWPA+SFS leads in efficiency, memory use, and simplicity.

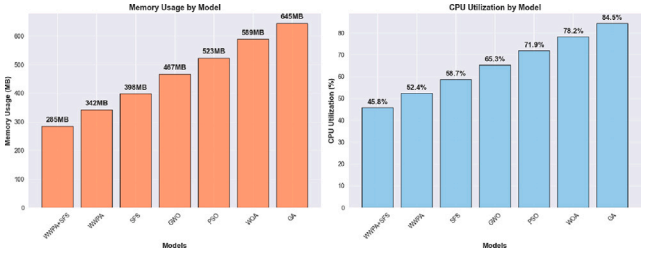

Fig. 35. Pareto Front (Left) and Accuracy vs Speed Trade-off (Right). WWPA+SFS dominates in both dimensions.

relative capabilities of several voting classifiers, including the proposed classifier, which assists in choosing the best classifier for the classification of heart attacks for women. The results indicate that the WWPA+SFS-based voting classifier outperforms other voting classifiers, which display significantly the best accuracy rate. The ANOVA and Wilcoxon Signed Rank Test results are essential statistical techniques to demonstrate the statistical significance of the suggested WWPA+SFS-based voting classifier. An evaluation of the voting classifier offered in this work will be carried out on various datasets in the future to identify the limitations and the improvements.

While this study is motivated by the need for improved diagnosis of heart attacks in women, a deeper gender-based comparative analysis was necessary to align with the title's focus. To address this, we performed a subgroup analysis across male and female patients in the dataset. The classifier's predictive behavior showed slight variations: models such as Logistic Regression and SVM achieved higher recall and precision metrics in the female subgroup, while models like Random Forest and k-NN maintained balanced performance across genders.

Furthermore, SHAP-based feature attribution analysis indicated that certain features—such as 'sex', 'chest pain type (cp)', and 'thalassemia (thall)'—interacted differently across genders. Specifically, the presence of atypical angina had a higher positive SHAP value in female patients, suggesting a stronger contribution to heart disease prediction in women. These nuances confirm that sex-specific patterns exist in the model's decision logic, underscoring the importance of gender-aware feature engineering.

These findings support the motivation for developing female-tailored prediction models and highlight the added value of explainable AI techniques in revealing sex-based differences. Future iterations of the study will stratify training and validation pipelines more explicitly by gender to further enhance the model's fairness and diagnostic specificity for women.

In terms of real-world applicability, the proposed WWPA+SFS voting classifier can be integrated into clinical decision support systems (CDSS) to assist cardiologists in triaging patients based on heart disease risk. By identifying subtle patterns in female-specific symptomatology, the model supports earlier interventions and reduces diagnostic delays—a common issue in women with ischemic heart disease.

From a deployment perspective, the model's computational efficiency and modular structure enable its adoption in both cloud-based hospital information systems and portable mobile health (mHealth) applications for remote diagnostics. Such applications are particularly beneficial in underserved or rural settings where access to cardiologists may be limited.

The study makes several key contributions: (1) it presents a novel hybrid optimization algorithm (WWPA+SFS) for feature-sensitive classification, (2) it integrates explainability tools such as SHAP for clinical interpretability, and (3) it performs gender-aware analysis to support the model's relevance for women's health—an area often overlooked in conventional research.

The significance of this study lies in its targeted approach to closing the diagnostic gap for women in cardiovascular care. By optimizing algorithmic precision and interpretability, this work supports evidence-based, equitable healthcare solutions that can have measurable impacts on mortality, cost, and quality of life.

6. Conclusion and future directions

This work presents a novel ensemble model—WWPA+SFS—that effectively combines the Waterwheel Plant Algorithm (WWPA) and Stochastic Fractal Search (SFS) for the classification of heart attacks in women using a machine learning voting scheme. The proposed classifier integrates multiple base learners including Logistic Regression, Gaussian Naive Bayes, Random Forest, Decision Tree, Stochastic Gradient Descent, k-nearest Neighbors, and Support Vector Classifier. Through rigorous evaluation, the model demonstrated superior predictive accuracy, robustness, and consistency when compared with several baseline optimization methods.

Key contributions of this study include: (1) the design of a synergistic WWPA+SFS optimization-driven voting classifier tailored to the female population, (2) statistical validation using ANOVA and Wilcoxon Signed Rank Test to establish significance, (3) implementation of 10-fold cross-validation to enhance generalizability, and (4) comparative performance analysis across various metaheuristic ensembles.

The experimental results confirm that the WWPA+SFS model offers an efficient solution to the complex task of heart attack prediction by exploiting complementary exploration and diffusion dynamics, outperforming other optimization algorithms in accuracy and stability.

For future directions, the research will focus on refining the proposed voting classifier, exploring additional optimization-based classifiers, and expanding the scope of health parameters for more robust heart attack classification models. Potential research will also examine the scalability of the model on larger, multi-institutional datasets and assess its clinical integration potential in decision-support systems. Subsequent studies will examine the application of the WWPA+SFS classifier to diverse healthcare datasets and its integration into real-world clinical settings, representing promising avenues for future research. The WWPA+SFS algorithm is planned to be compared with a wide range of recent algorithms rather than the original WWPA algorithm.

CRediT authorship contribution statement

Doaa Sami Khafaga: Writing – original draft, Visualization, Software, Methodology, Formal analysis, Conceptualization. **Marwa M. Eid:** Writing – original draft, Data curation. **El-Sayed M. El-kenawy:** Writing – review & editing, Validation. **Ehsaneh Khodadadi:** Writing – review & editing, Validation. **Amel Ali Alhussan:** Writing – review & editing, Visualization. **Nima Khodadadi:** Writing – review & editing, Supervision, Project administration.

Ethical approval

This study does not require ethical approval. Consent to publication All authors read and approved the final manuscript.

Declaration of competing interest

The authors declare that they have no known competing financial interests or personal relationships that could have appeared to influence the work reported in this paper.

Acknowledgments

Princess Nourah bint Abdulrahman University Researchers Supporting Project number (PNURSP2025R754), Princess Nourah bint Abdulrahman University, Riyadh, Saudi Arabia.

Data availability

The data that support the findings of this study are openly available in kaggle at [https://www.kaggle.com/datasets/rashikrahmanpritom/heart-attack-analysis-prediction-dataset].

References

[1] E.G. Giardina, Heart disease in women, Int. J. Fertil. Women's Med. 45 (6) (2000) 350–357, https://pubmed.ncbi.nlm.nih.gov/11140544/.

[2] C.M. Otto, Heartbeat: focus on heart disease in women, Heart 106 (7) (2020) 477–478, http://dx.doi.org/10.1136/heartjnl-2020-316802.

[3] S.N. Gowda, S.s. Garapati, K. Kurrelmeyer, Spectrum of ischemic heart disease throughout a woman's life cycle, Methodist DeBakey Cardiovasc. J. 20 (2) (2024) 81–93, http://dx.doi.org/10.14797/mdcvj.1331.

[4] S. Ranasinghe, et al., Elevated high-density lipoprotein cholesterol and adverse outcomes in women with symptoms of ischemic heart disease, Am. Hear. J. Plus Cardiol. Res. Pr. 40 (2024) 100376, http://dx.doi.org/10.1016/j.ahjo.2024.100376.

[5] N.K. Wenger, The feminine face of heart disease 2024, Circulation 149 (7) (2024) 489–491, http://dx.doi.org/10.1161/circulationaha.123.064460.

[6] S. Steinbaum, The future of women and heart disease in a pandemic era: Let's learn from the past, Medicina 57 (5) (2021) 467, http://dx.doi.org/10.3390/medicina57050467.

[7] M.I. Hossain, et al., Heart disease prediction using distinct artificial intelligence techniques: performance analysis and comparison, Iran J. Comput. Sci. 6 (4) (2023) 397–417, http://dx.doi.org/10.1007/s42044-023-00148-7.

[8] G.H. Tison, et al., Predicting incident heart failure in women with machine learning: The women's health initiative cohort, Can. J. Cardiol. 37 (11) (2021) 1708–1714, http://dx.doi.org/10.1016/j.cjca.2021.08.006.

[9] A. Ogunpola, F. Saeed, S. Basurra, A.M. Albarrak, S.N. Qasem, Machine learning-based predictive models for detection of cardiovascular diseases, Diagnostics 14 (2) (2024) 144, http://dx.doi.org/10.3390/diagnostics14020144.

[10] S. Gangadharan, et al., Comparative analysis of deep learning-based brain tumor prediction models using MRI scan, in: 2023 3rd International Conference on Innovative Sustainable Computational Technologies, CISCT, IEEE, 2023, pp. 1–6.

[11] M. Diwakar, P. Singh, D. Garg, Edge-guided filtering based CT image denoising using fractional order total variation, Biomed. Signal Process. Control. 92 (2024) 106072.

[12] M. Diwakar, P. Kumar, P. Singh, A. Tripathi, L. Singh, An efficient reversible data hiding using SVD over a novel weighted iterative anisotropic total variation based denoised medical images, Biomed. Signal Process. Control. 82 (2023) 104563.

[13] M. Diwakar, et al., Low-dose COVID-19 CT image denoising using CNN and its method noise thresholding, Curr. Med. Imaging Rev. 19 (2) (2023) 182–193.

[14] T. Agrawal, P. Choudhary, A. Shankar, P. Singh, M. Diwakar, MultiFeNet: Multi-scale feature scaling in deep neural network for the brain tumour classification in MRI images, Int. J. Imaging Syst. Technol. 34 (1) (2024) e22956.

[15] H. Nasser AlEisa, et al., Transfer learning for chest X-rays diagnosis using dipper throated algorithm, Comput. Mater. Contin. 73 (2) (2022) 2371–2387, http://dx.doi.org/10.32604/cmc.2022.030447.

[16] A.A. Alhussan, et al., Classification of diabetes using feature selection and hybrid Al-Biruni earth radius and dipper throated optimization, Diagnostics 13 (12) (2023) 2038, http://dx.doi.org/10.3390/diagnostics13122038, URL https://www.mdpi.com/2075-4418/13/12/2038.

[17] W.-Y. Lin, A novel 3D fruit fly optimization algorithm and its applications in economics, Neural Comput. Appl. 27 (5) (2015) 1391–1413, http://dx.doi.org/10.1007/s00521-015-1942-8.

[18] X. Wang, T.-M. Choi, H. Liu, X. Yue, A novel hybrid ant colony optimization algorithm for emergency transportation problems during post-disaster scenarios, IEEE Trans. Syst. Man Cybern. Syst. 48 (4) (2018) 545–556, http://dx.doi.org/10.1109/tsmc.2016.2606440.

[19] R.V. Rao, G. Waghmare, A new optimization algorithm for solving complex constrained design optimization problems, Eng. Optim. 49 (1) (2016) 60–83, http://dx.doi.org/10.1080/0305215x.2016.1164855.

[20] R. Bello, Y. Gomez, A. Nowe, M.M. Garcia, Two-step particle swarm optimization to solve the feature selection problem, in: Seventh International Conference on Intelligent Systems Design and Applications, ISDA 2007, 2007, pp. 691–696, http://dx.doi.org/10.1109/ISDA.2007.101.

[21] A.T. Mozhdehi, N. Khodadadi, M. Aboutalebi, E.-S.M. El-kenawy, A.G. Hussien, W. Zhao, M.H. Nadimi-Shahraki, S. Mirjalili, Divine religions algorithm: a novel social-inspired metaheuristic algorithm for engineering and continuous optimization problems, Cluster Comput. 28 (4) (2025) 253, http://dx.doi.org/10.1007/s10586-024-04954-x.

[22] E. Rashedi, H. Nezamabadi-pour, S. Saryazdi, GSA: A gravitational search algorithm, Inform. Sci. 179 (13) (2009) 2232–2248, http://dx.doi.org/10.1016/j.ins.2009.03.004.

[23] S. Mirjalili, S.M. Mirjalili, A. Lewis, Grey wolf optimizer, Adv. Eng. Softw. 69 (2014) 46–61, http://dx.doi.org/10.1016/j.advengsoft.2013.12.007.

[24] D.S. Khafaga, et al., An Al-Biruni earth radius optimization-based deep convolutional neural network for classifying monkeypox disease, Diagnostics 12 (11) (2022) 2892, http://dx.doi.org/10.3390/diagnostics12112892.

[25] J.H. Holland, Genetic algorithms, Sci. Am. 267 (1) (1992) 66–73.

[26] A.A. Abdelhamid, et al., Waterwheel plant algorithm: A novel metaheuristic optimization method, Processes 11 (5) (2023) 1502, http://dx.doi.org/10.3390/pr11051502.

[27] B. Abdollahzadeh, N. Khodadadi, S. Barshandeh, P. Trojovskỳ, F.S. Gharehchopogh, E.-S.M. El-kenawy, L. Abualigah, S. Mirjalili, Puma optimizer (PO): a novel metaheuristic optimization algorithm and its application in machine learning, Cluster Comput. 27 (4) (2024) 5235–5283, http://dx.doi.org/10.1007/s10586-023-04221-5.

[28] M.H. Amiri, N. Mehrabi Hashjin, M. Montazeri, S. Mirjalili, N. Khodadadi, Hippopotamus optimization algorithm: a novel nature-inspired optimization algorithm, Scient. Rep. 14 (1) (2024) 5032, http://dx.doi.org/10.1038/s41598-024-54910-3.

[29] W. Zhao, L. Wang, Z. Zhang, H. Fan, J. Zhang, S. Mirjalili, N. Khodadadi, Q. Cao, Electric eel foraging optimization: A new bio-inspired optimizer for engineering applications, Expert Syst. Appl. 238 (2024) 122200, http://dx.doi.org/10.1016/j.eswa.2023.122200.

[30] L. Wang, H. Du, Z. Zhang, G. Hu, S. Mirjalili, N. Khodadadi, A.G. Hussien, Y. Liao, W. Zhao, Tianji's horse racing optimization (THRO): a new metaheuristic inspired by ancient wisdom and its engineering optimization applications, Artificial Intell. Rev. 58 (9) (2025) 1–111, http://dx.doi.org/10.1007/s10462-025-11269-9.

[31] A. Kaveh, S. Talatahari, N. Khodadadi, Stochastic paint optimizer: theory and application in civil engineering, Eng. Comput. 1–32, http://dx.doi.org/10.1007/s00366-020-01179-5.

[32] R. Aggrawal, S. Pal, Sequential feature selection and machine learning algorithm-based patient's death events prediction and diagnosis in heart disease, SN Comput. Sci. 1 (6) (2020) http://dx.doi.org/10.1007/s42979-020-00370-1.

[33] M.M. Ali, et al., Heart disease prediction using supervised machine learning algorithms: Performance analysis and comparison, Comput. Biol. Med. 136 (2021) 104672, http://dx.doi.org/10.1016/j.compbiomed.2021.104672.

[34] A. Banerjee, et al., Machine learning for subtype definition and risk prediction in heart failure, acute coronary syndromes and atrial fibrillation: systematic review of validity and clinical utility, BMC Med. 19 (1) (2021) http://dx.doi.org/10.1186/s12916-021-01940-7.

[35] G. Bazoukis, et al., Machine learning versus conventional clinical methods in guiding management of heart failure patients—a systematic review, Heart Fail. Rev. 26 (1) (2020) 23–34, http://dx.doi.org/10.1007/s10741-020-10007-3.

[36] V. Chang, V.R. Bhavani, A.Q. Xu, M. Hossain, An artificial intelligence model for heart disease detection using machine learning algorithms, Heal. Anal. 2 (2022) 100016, http://dx.doi.org/10.1016/j.health.2022.100016.

[37] D. Chicco, G. Jurman, Machine learning can predict survival of patients with heart failure from serum creatinine and ejection fraction alone, BMC Med. Inform. Decis. Mak. 20 (1) (2020) http://dx.doi.org/10.1186/s12911-020-1023-5.

[38] K. Divya, A. Sirohi, S. Pande, R. Malik, An IoMT assisted heart disease diagnostic system using machine learning techniques, in: Studies in Systems, Decision and Control, Springer International Publishing, 2020, pp. 145–161, http://dx.doi.org/10.1007/978-3-030-55833-8_9.

[39] H. Jiang, et al., Machine learning-based models to support decision-making in emergency department triage for patients with suspected cardiovascular disease, Int. J. Med. Inform. 145 (2021) 104326, http://dx.doi.org/10.1016/j.ijmedinf.2020.104326.

[40] P. Sharma, et al., Artificial plant optimization algorithm to detect heart rate & presence of heart disease using machine learning, Artif. Intell. Med. 102 (2020) 101752, http://dx.doi.org/10.1016/j.artmed.2019.101752.

[41] K. Wang, et al., Interpretable prediction of 3-year all-cause mortality in patients with heart failure caused by coronary heart disease based on machine learning and SHAP, Comput. Biol. Med. 137 (2021) 104813, http://dx.doi.org/10.1016/j.compbiomed.2021.104813, URL http://dx.doi.org/10.1016/j.compbiomed.2021.104813.

[42] R. Rahman, Heart attack analysis & prediction dataset: A dataset for heart attack classification, 2021, URL https://www.kaggle.com/datasets/rashikrahmanpritom/heart-attack-analysis-prediction-dataset.

[43] A. Fatchul Huda, A. Solih Awalluddin, Y. Dwi Lestari, F. Muhtarulloh, Gaussian kernel naïve Bayes classifier on hadith corpus, in: 2023 9th International Conference on Wireless and Telematics, ICWT, IEEE, 2023, http://dx.doi.org/10.1109/icwt58823.2023.10335392.

[44] T. Haifley, Linear logistic regression: an introduction, in: IEEE International Integrated Reliability Workshop Final Report, 2002, in: IRWS-02, IEEE, http://dx.doi.org/10.1109/irws.2002.1194264.

[45] U.N. A, K. Dharmarajan, Diabetes prediction using random forest classifier with different wrapper methods, in: 2022 International Conference on Edge Computing and Applications, ICECAA, IEEE, 2022, http://dx.doi.org/10.1109/icecaa55415.2022.9936172.

[46] W. Guo, A gradient-descent-based k-NN algorithm, 2022, http://dx.doi.org/10.31219/osf.io/kqdxu, Preprint on OSF.

[47] S. Sameer, P. Sriramya, Improving the accuracy for prediction of heart disease by novel feature selection scheme using decision tree comparing with naive-Bayes classifier algorithms, in: 2022 International Conference on Business Analytics for Technology and Security, ICBATS, IEEE, 2022, http://dx.doi.org/10.1109/icbats54253.2022.9758926.

[48] G. Wen-wen, Y. Lv, Y. Jia-yu, Z. Wang, S. Yuan-hai, Fast support vector classifier with generalization-memorization kernel, Procedia Comput. Sci. 214 (2022) 55–62, http://dx.doi.org/10.1016/j.procs.2022.11.148.

[49] S. Charan, S. M.S, S. R, Prediction of insufficient accuracy for human activity recognition with limited range of age using K-nearest neighbor, in: 2023 Second International Conference on Electronics and Renewable Systems, ICEARS, IEEE, 2023, http://dx.doi.org/10.1109/icears56392.2023.10085062.